LUT UNIVERSITY
LUT School of Energy Systems
LUT Mechanical Engineering

Topias Parviainen

DESIGN AND SIMULATION OF SQUEEZE FILM DAMPERS IN TEST RIG

13.11.2019
Examiners: Prof. Jussi Sopanen
D. Sc. (Tech.) Eerik Sikanen

TIIVISTELMÄ

LUT-Yliopisto
LUT School of Energy Systems
LUT Kone

Topias Parviainen

Design and simulation of squeeze film dampers in test rig

Diplomityö

2019

62 sivua, 37 kuvaa, 17 taulukkoa ja 2 liitettä

Tarkastajat: Prof. Jussi Sopanen
TkT Eerik Sikanen

Hakusanat: Roottoridynamiikka, Numeerinen mallinnus, Öljykalvovaimennin, Modulaarinen suunnittelu, Integroitu öljykalvovaimennin

Tutkimuksen tavoitteena oli suunnitella roottorin testauslaitteeseen öljykalvovaimentimet ja tutkia niiden käyttäytymistä virtuaalimallissa. Testiroottori mallinnettiin MATLAB:in Rotor-Bearing Dynamics-paketin (RoBeDyn-paketin) avulla, aluksi ilman vaimentimia. Mallissa on tässä vaiheessa kuusi massapistettä ja 21 solmua. Malli verifioitiin vertaamalla sen avulla saatuja tuloksia testiroottoriin tehtyihin mittauksiin. Mittaukset tehtiin 1D-piezoantureilla ja niiden avulla mitattiin kiihtyvyyksiä aikatasossa testiroottorista sen ollessa pyörimättä. Saadut tulokset muunnettiin Fast Fourier Transform-muunnoksella (FFT-muunnoksella) aikatasosta taajuustasoon ja niitä verrattiin numeerisen mallin vastaaviin tuloksiin.

Tehtyyn numeeriseen malliin lisättiin öljykalvovaimentimet. Mallissa oli tässä vaiheessa kahdeksan massapistettä ja 23 solmua. Vaihtelemalla vaimentimien jäykkyyttä ja vaimennusta, etsittiin arvot, joilla värähtelyamplitudi ennalta valitussa kolmessa pisteessä oli mahdollisimman pieni. Näiden saatujen numeeristen arvojen avulla alettiin suunnitella 3D-osia vaimentimille. Suunnitelluista öljykalvovaimentimista, sopivimmaksi todettiin nelijousinen vaimennin. Sen jäykkyys, vaimennus ja fyysiset mitat vastasivat numeerisen mallin avulla etsittyjä lukuarvoja. Suunnitellut vaimentimet mahtuvat alkuperäiseen laakeripesään, ovat modulaarinen yksikkö ja ne on helppo vaihtaa tai ottaa pois, mikä tukee työhön kuuluvaa modulaarista suunnittelua.

Suunnitellut vaimentimet pienensivät selvästi resonanssin aiheuttamaa äkillistä muutosta värähtelyamplitudissa, ja resonanssin aiheuttama värähtelypiikki vaimeni leviten laajemmalle alueelle. Vertaamalla Campbell diagrammia testiroottorista ilman vaimentimia ja vaimentimien kanssa huomattiin, että vaimentimet laskevat roottorin resonanssitaajuuksia. Suunnitellut vaimentimet toimivat odotetulla tavalla.

ABSTRACT

LUT University
LUT School of Energy Systems
LUT Mechanical Engineering

Topias Parviainen

Design and simulation of squeeze film dampers in test rig

Master's thesis

2019

62 pages, 37 figures, 17 tables and 2 appendices

Examiners: Prof. Jussi Sopanen
D. Sc. (Tech.) Eerik Sikanen

Keywords: Rotor dynamics, Numerical modelling, Squeeze film damper, Modular design, Integral squeeze film damper

The goal of the research was to design Squeeze Film Dampers (SFDs) into the test rig and study their behavior in virtual model of the rig. The test rotor was modelled with MATLABs RoBeDyn-toolbox, first without the dampers. At this point, there are six mass points and 21 nodes in model. The model was verified by comparing the results from numerical model to results from done measurements from the test rotor. Measurements were done with 1D piezo sensors and they were used to measure accelerations in time domain on test rotor while it was stationary. Gained results were converted from time domain to frequency with FFT-method and the results were compared to numerical model's same situation results.

Dampers were added into the numerical model. There are, at this point, eight mass points and 23 nodes in model. Damping and stiffness of dampers was adjusted so that, vibration amplitude reached its minimum value. With these parameters, the designing of the dampers began. From designed dampers, model with four-springs was found out the most suitable. It's stiffness, damping and dimensions were close to the ones from numerical model. Designed dampers fit into the original bearing housing, they are modular unit and they are easy to assemble or disassemble, which supports the modular design view.

The designed SFDs clearly lowered the amplitude in resonance frequencies, and they spread the resonance spike into wider range of Revolutions Per Minutes (RPMs) with their damping ability. By comparing the Campbell diagram of the test rig without and with SFDs, we noticed that the SFDs are lowering resonance frequencies on the test rig. The SFDs are working in model as they were expected to work.

TABLE OF CONTENTS

LIST OF SYMBOLS

Roman alphabets

C	Global damping Matrix
c_c	Squeeze film damper radial clearance [m]
C_{SFD}	Damping of squeeze film damper [Ns/m]
c_Y	Damping in *Y*-direction [Ns/m]
c_Z	Damping in *Z*-direction [Ns/m]
d_{in}	Inner diameter [m]
d_{out}	Outer diameter [m]
E	Elastic modulus [Pa]
f	Frequency [Hz]
$\boldsymbol{F}$	Nodal force vector
F_Y	Force in *Y*-direction [N]
F_Z	Force in *Z*-direction [N]
G	Gyroscopic moment matrix of rotating disc
h	Mass point offset [m]
i	Number of modes [no unit]
I_p	Polar inertia [kg·m^2]
J_{xx}	Mass moment of inertia in *xx*-direction [kg·m^2]
J_{yy}	Mass moment of inertia in *yy*-direction [kg·m^2]
J_{zz}	Mass moment of inertia in *zz*-direction [kg·m^2]
k	Stiffness [N/m]
K	Global stiffness matrix
k_{SFDy}	Stiffness on squeeze film damper in *Y*-direction [N/m]
k_{SFDz}	Stiffness on squeeze film damper in *Z*-direction [N/m]
K_Y	Stiffness in *Y*-direction [N/m]
K_Z	Stiffness in *Z*-direction [N/m]
k_s	Shear correction factor [no unit]
L	Length of squeeze film damper [m]
m	Unbalanced mass in disc [kg]

$\mathbf{M}$	Mass matrix of test rotor
n	Amount of springs [no unit]
$\boldsymbol{q}$	Vector of nodal displacement
$\dot{\boldsymbol{q}}$	Vector of nodal velocity
$\ddot{\boldsymbol{q}}$	Vector of nodal acceleration
r	Radial distance of unbalanced mass [m]
rho	Density of material [kg/m^3]
R	Radius of squeeze film damper [m]
R_1	Radius of first oil film [m]
R_2	Radius of second oil film [m]
t	Time [s]
U_Y	Displacement in Y-direction [mm]
U_Z	Displacement in Z-direction [mm]

Greek alphabets

α	Angle of unbalance [rad]
η	Oil viscosity [Pa·s]
v	Poisson's ratio [no unit]
Ω	Angular velocity [rad/s]

LIST OF ABBREVIATIONS

AMB	Active Magnetic Bearing
BW	Backward Whirling
ISFD	Integral Squeeze Film Damper
FEM	Finite Element Method
FFT	Fast Fourier Transform
FW	Forward Whirling
MDOF	Multi Degree of Freedom
RAMBO	Reippaaseen kasvuun AMB-Osaamisella
RoBeDyn	Rotor-Bearing Dynamics
RPM	Revolutions Per Minute
SFD	Squeeze Film Damper

1 INTRODUCTION

Active Magnetic Bearings (AMB) are used to support any ferromagnetic bodies, such like shafts, without any contact. The advantage of using AMBs is that there is no need for lubrication in bearing and there is no mechanical wear in bearings, because there is no contact to shaft (Larsonneur 1990, p. 1). The disadvantage of using AMBs is that they require more space than the traditional bearings do. Also, if there is power shortage, the AMBs stop operating. If AMBs stop operating, there is nothing that will support the shaft. Safety bearings are needed, when AMBs fail operating. Safety bearings will catch the shaft and safely let it slow down if AMBs suddenly stop operating.

“Reippaaseen kasvuun AMB-osaamisella”-project (RAMBO-project) aimed for researching and testing AMBs. The AMB test rig, built for RAMBO-project, is in Lappeenranta, and it was created for testing magnetic bearings in RAMBO-project. The test rig can be seen in figure 1. For later usage, the test rig will be modified having possibility to be operated without AMBs. This will be done by operating test rig with AMBs safety bearings. However, there is need for damping on this option, so the test rig will be needing a damping unit on it. The damping will be achieved by using squeeze film dampers. Idea of squeeze film damper is a film of oil that absorbs vibration energy. Oil in SFD is used to dampen the vibrations that are coming from bearing-bearing system (Goodwin 1989, p. 48-49). There is also need for numerically modelling the test rig and its components to study its dynamical behavior without and with SFDs and for later uses as well.

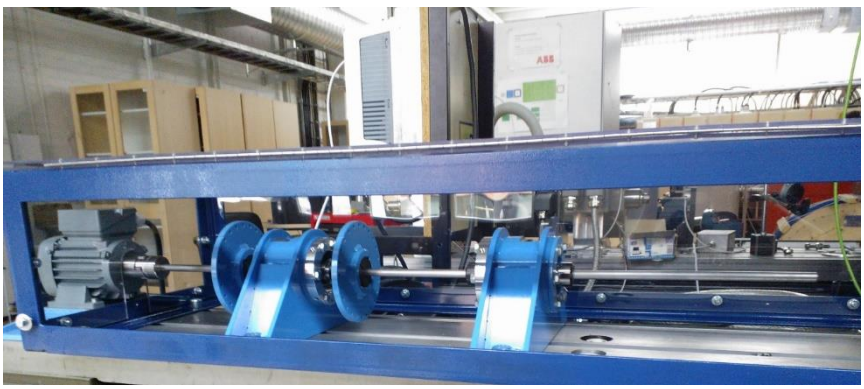

Figure 1. The AMB test rig of this project.

There have been some similar researches lately. There has been an experimental research on a test bench with bearings and squeeze film dampers for developing the test bench. The study showed that SFDs caused nonlinear behavior in system and rattle in bearings. (Meesus & al 2019). There was a study about magnetorheological SFDs on a Jeffcott rotor. That study contained also mathematical modeling of the test rig they used in study. Study showed that the magnetorheological fluids in SFDs, reduced the nonlinear behavior in SFDs. Also, the done mathematical model proved the results from done study correct. (Zapoměl, Ferfecki, & Forte 2019). There was a study done with Integral Squeeze Film Dampers (ISFDs) on a gear shaft with misalignments. Experiments showed that ISFDs were excellent solution for reducing vibrations and making the system more controllable. (Lu & al 2019).

1.1 Background

This research is done after the RAMBO-project was finished. The RAMBO-project aimed for developing cost efficient inductive location sensor, cost efficient magnetic bearing controller and advanced electro-mechanic safety bearing for rotating high-speed electrical machines. The test rig was created as a part of testing inductive location sensors (Sikanen 2019a). This research is going to continue developing the test rotor, which was originally built for RAMBO-project. The test rotor will be numerically modelled for studying its dynamic behavior. Also, SFDs will be designed for test rotor and they will be added into the numerical model of test rotor and their effect into model's dynamical behavior will be studied.

1.2 Goals, hypothesis and scope

The purpose of this research is to design modular SFD-units for the test rig and create numerical model of test rig to predict its dynamical behavior. The numerical model can be used for estimating dynamical behavior of test rig with different kinds of damping units. By using the numerical model as estimation tool, ideal values for dampers in test rig can be found. Numerical model can also be modified for different set ups of test rig. For example, with more components or with different locations for its components or with different supports.

1.2.1 Research problems

LUT-university's laboratory of Machine Dynamics is interested to modify the RAMBO-test rig on teaching purposes. The properties of test rig need to be easily modified. The properties can be for example adjusting the amount of unbalance, adjusting stiffness or adjusting damping in the rig or in its supports. On this research, we are especially interested about adjusting the damping on test rig.

Numerical model can be used to predict test rigs behavior with different set ups. That can be done by using, for example MATLAB, to create numerical model of the test rig. Numerical model needs to be verified by comparing results from numerical model to results gained from measurements with same settings than the numerical model was simulated with. When the numerical model is working properly, it can be used for estimating parameters for SFDs. Gained parameters can be used for calculating dimensions for SFDs and after having dimensions for dampers, they can be modelled in 3D-modelling software.

The aim of this research is to answer on following research questions:

- How is the test rig behaving on different frequencies before it has SFDs?
- What are required parameters for modelling SFDs and what are optimal values for those parameters?
- How the SFDs can be designed so they can be fitted in test rig as modular units?
- How is the test rig behaving on different frequencies with SFDs?
- What SFDs are changing in dynamical behavior of test rig compared to the rig without SFDs?

1.2.2 Hypothesis

The hypothesis of this research is that parameters for modelling SFDs can be found by using numerical model. Dimensions in SolidWorks model are assumed to be accurate enough to be used in numerical modelling. SFDs are assumed to lower resonance frequencies and reduce amplitude of vibration. Also, it is assumed that the modular damping unit can be designed by using found parameters of SFDs and by using the 3D-model of test rig.

1.2.3 Scope

This research is limited to creating numerical model of test rig and researching rigs vibrations. Numerical modelling will be done using MATLAB-software. Data used in numerical modelling will be based on SolidWorks model of test rig and on data from measuring the locations of components in particular configuration in test rig. Model will be verified by comparing results from done numerical model to results from vibration measurements done with the test rig that locates in LUT-university.

1.3 Structure of the thesis

This thesis introduces rotor dynamics, SFD-theory, vibration measurements, numerical modelling of rotor-bearing-dynamic system and modular designing of damping unit. Section 2 familiarizes the reader with theory and literature findings of rotor dynamics, SFD-theory and vibration measurement theory. Section 3 introduces the reader with test rig, numerical modelling parameters for test rigs components, building the numerical model and how parameters for SFDs were found. Section 4 shows the results from test rig first without SFDs, modelled SFDs and their properties, results from test rig with SFDs and results from done measurements. Section 5 has comparison and discussion of gained results from test rig with and without SFDs and comparing results from numerical model to results from measurements. There is also discussion about accuracy, sensitivity, reliability and validity of done numerical model. There’s also discussion about success of modular designing of SFDs. Section 6 summarizes the done research.

2 ROTOR DYNAMICS AND SQUEEZE FILM DAMPERS

On this section, we discuss about the methods used to carry out this research. First, there is literature review about two main topics in this research: rotor dynamics and squeeze film dampers. In rotor dynamic part, we discuss about basics of that topics, need for rotor dynamic research, resonating, some equations that define rotor dynamic systems and how to calculate natural frequencies of rotor dynamic systems. In SFD part, we discuss about basics of SFDs, how to calculate their damping and what parameters we need to know for that and some discussion about special type of SFD, that could be useful in this research. Finally, there is some theory about vibration measurements. All numerical modelling will be based to findings from the literature.

2.1 Rotor dynamics

Rotor dynamics analyze and determinate dynamic behavior with modern methods and modelling software's. Modern methods for analyzing dynamic behavior are calculation software's, for example MATLAB (Friswell, Penny, Garvey & Lees 2010, p. 1). Rotating particles are the most often the cause of vibrations in machines or in systems. With correct knowledge and methods, the vibrations can be eliminated or can be made so small, that they do not matter (Yamamoto & Ishida 2001, p. xvii).

Term rotor is often used from a part in machinery that rotates. The geometry of rotor can be any. With complex shapes of rotor, the rotor needs to be simplified to a simpler geometry, when using beam elements research the rotor (Yamamoto & Ishida 2001, p. 1). Reducing the model can be achieved by reducing features from rotors geometry (Airila & al 1985, p. 320-321). The properties of rotor, bearings and supports define systems critical speed. The properties that effect to the critical speeds are the stiffness, the mass and the gyroscopic effects of the rotor, bearings and supports. When the rotor hits the critical speed, system starts to resonate and create vibrations that may cause problems. The problems can be for example: wear in bearings, failure in seals, the vibrations might be transmitted to the supports and that may cause breaking of the supports or noise (Friswell, Penny, Garvey & Lees 2010, p. 1).

The system in rotor dynamics consists from rotating discs, elastic shafts with mass and from their supports, for example from bearings. This method is called as lumped mass method. The unbalanced mass in discs is marked as *m* and the radius for that from the center line is marked as *e* (Yamamoto & Ishida 2001, p. 6-7). Figure 2 shows those parameters and their meanings more clearly.

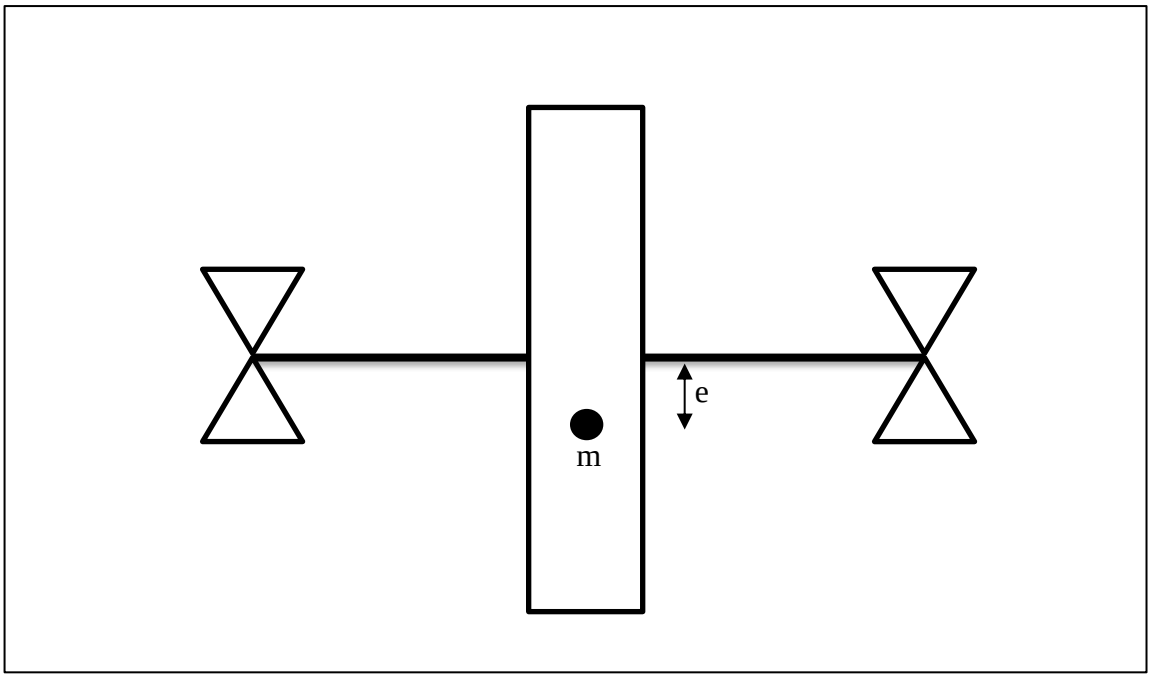

Figure 2. Unbalanced mass and its distance from center line in rotating system. *m* is the unbalanced mass and *e* is the radius for unbalanced mass from the center line.

Equation of motion for multiple-degree-of-freedom system can be defined by using following equation (Friswell, Penny, Garvey & Lees 2010, p. 34-35).:

$$\mathbf{M}\ddot{\boldsymbol{q}} + \mathbf{C}\dot{\boldsymbol{q}} + \mathbf{K}\boldsymbol{q} = \boldsymbol{F} \qquad (1)$$

In equation 1, **M** is the mass matrix of the rotor system, **C** is global damping matrix of rotor system **K** is the global stiffness matrix of rotor system, $\boldsymbol{q}$ is vector of nodal coordinates, $\dot{\boldsymbol{q}}$ vector of nodal velocity, $\ddot{\boldsymbol{q}}$ is vector of nodal acceleration and $\boldsymbol{F}$ is vector of nodal force. **K** and **M** can be gained by calculating them using proper equations, but they can be gained also using 3D-modelling software (Genta 2005, p. 155).

For rotating system gyroscopic effects need to be taken account. Following equation shows gyroscopic moment matrix for rotating disc with six degrees of freedom (Friswell, Penny, Garvey & Lees 2010, p. 97).:

$$\mathbf{G} = \begin{bmatrix} 0 & 0 & 0 & 0 & 0 & 0 \\ 0 & 0 & 0 & 0 & 0 & 0 \\ 0 & 0 & 0 & 0 & 0 & 0 \\ 0 & 0 & 0 & 0 & 0 & 0 \\ 0 & 0 & 0 & 0 & 0 & I_p \\ 0 & 0 & 0 & 0 & -I_p & 0 \end{bmatrix} \tag{2}$$

In equation 2, **G** is the gyroscopic moment matrix of rotating disc and I_p is polar moment. Gyroscopic terms are affecting imaginary parts of rotors eigenfrequencies. They split rotors eigenmodes to ascending and descending imaginary parts. These imaginary parts define rotors forward and backward modes. The real parts of rotors eigenfrequencies define stability of rotor. (Larsonneur 1990, p. 111-112). Terms in gyroscopic moment matrix are functions of rotation speed. If rotation speed is zero, terms in gyroscopic moment matrix are zero. (Genta 2005, p. 6).

By combining equation 1 and equation 2, we get following equation as equation of motion for test rotor (Nässelqvist 2009).:

$$\mathbf{M}\ddot{\boldsymbol{q}} + \dot{\boldsymbol{q}}(\boldsymbol{C} + \Omega\mathbf{G}) + \mathbf{K}\boldsymbol{q} = \boldsymbol{F} \tag{3}$$

Ω is the angular velocity in equation 3. Equation 3 can be used for solving systems displacement as a function of rotation speed on a prechosen point.

Unbalanced masses in rotor cause forces, which will make the rotor deform while rotating. These forces can be calculated as function of time, if we know proper parameters about unbalance in rotor. Following equation shows, how the unbalance in *Y*- and *Z*-direction can be calculated (Sopanen & al 2019, p. 38).:

$$\begin{bmatrix} F_Y \\ F_Z \end{bmatrix} = m \cdot e \cdot \Omega^2 \begin{bmatrix} -\sin(\alpha) \\ \cos(\alpha) \end{bmatrix} \cdot \sin(\Omega \cdot t) + m \cdot e \cdot \Omega^2 \begin{bmatrix} \cos(\alpha) \\ \sin(\alpha) \end{bmatrix} \cdot \cos(\Omega \cdot t) \qquad (4)$$

In equation 4, F_Y is force in Y-direction, F_Z is force in Z-direction, α is the angle of unbalance and t is time. By combining equation 3 and 4, we can solve system unbalance. Unbalance response is showing vibration amplitude in a prechosen point as a function of rotation speed. This method can be used for example, finding resonance frequencies of system while it is being operated.

Campbell diagram is showing natural frequencies and damping ratios as a function of rotation speed. Matrices for calculating Campbell diagram are depending from rotors rotation speed. For creating Campbell diagram, all rotation speed dependent values need to be calculated step by step to wanted maximum frequency and then solving eigen value problem for each used step. Critical speeds in Campbell diagram can be found, when natural frequency of rotor is crossing the rotation speed. (Sopanen & al 2019, p. 36-37).

2.2 Squeeze film damper- theory

Hydrodynamic bearings are bearings that do not have rolling elements, but instead of them they have a thin film of oil pumped between bearings outer and inner layer. The oil film is called hydrodynamic oil film. The oil film is used to reduce the friction between shaft and supports, because the oil film has very low friction factor. Squeeze film dampers are type of hydrodynamic bearings. However, SDFs usually are not rotating. (Friswell, Penny, Garvey & Lees 2010, p. 176-189).

Idea of squeeze film damper is a film of oil being supplied between a bearing holder and bearing case. Oil in SFD is used to dampen the vibrations that are transmitted through the bearing. The SFDs are especially effective, when the machine is close operating at the critical speeds. It is possible to have pressurized oil in SFD or not pressurized oil in SFD. There can be fitted seals in SFD, so the oil would not leak out from the SFD. Because SFDs are not rotating, they have low hydrodynamic stiffness and so no capability to carry static loads, so there can be a centralizing spring on damper that minimizes the effect of static loads and the bearing contacting the bearing case. SFDs are mostly used with bearings with rolling elements, because rolling elements in bearings have very low damping. Figure 3 is showing

SFD and its different components. (Yamamoto & Ishida 2001, p. 114-115, Goodwin 1989, p. 48-49, Friswell, Penny, Garvey & Lees 2010, p. 189).

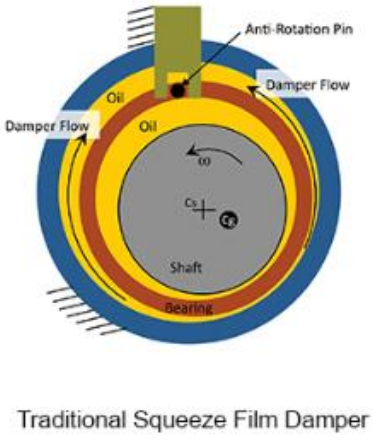

Figure 3. Squeeze film damper and its components. (Waukesha Bearings 2019a).

The damping of SFD can be calculated from following equation (Friswell, Penny, Garvey & Lees 2010, p. 190-191).:

$$C_{SFD} = \frac{\pi \cdot \eta \cdot R \cdot L^3}{2 \cdot {c_c}^3} \tag{5}$$

In equation 5 C_{SFD} is the damping of squeeze film damper, η is oil viscosity, R is the radius of the damper, L is the damper length and c_c is the dampers radial clearance.

When taking account that we are using SFDs and roller bearings, ISDFs could be useful by their ability to be fitted directly around existing bearings. ISFDs are sheet metal structures filled with oil. The picture of ISFD can be seen in figure 4. This is space saving method and this solution would not require pump for lubricating oil (Waukesha Bearings 2019b). ISFD would also be good solution by thinking the modular design point of view. By adjusting thickness or thicknesses of SFD and thickness of oil film in SFD and by adjusting the amount and thickness of springs in SFD, the properties of SFD can be adjusted.

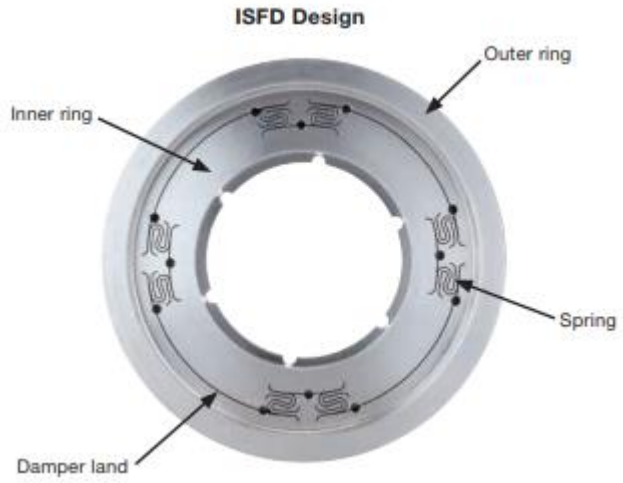

Figure 4. Integral squeeze film dampers. (Waukesha Bearings 2019c).

2.3 Measuring methods theory

Vibrations from rotating machinery need to be measured, so we can monitor the condition of the machine. We also sometimes might need to find out resonance frequencies by doing measurements. High levels of vibrations cause stress on machines components and can cause a lot of noise or a failure of a component. Measurement data is usually visualized by showing system's amplitude as function of rotation speed or frequency (Goodwin 1989, p. 248-249). This visualization is called as unbalance response. Measured data can also be shown in time domain. Time domain shows vibration amplitude as a function of time.

Piezo sensor measures acceleration in one direction from set point. These sensors create a small signal voltage as a function of acceleration during measurement. This signal, however, needs to be amplified so it can be used for visualizing the results. Amplified voltage signals from amplifier can be visualized for example with oscilloscopes, with spectrum analyzers or with tracking filters. These methods can be also used for transforming measured data in different form. (Goodwin 1989, p. 248-249).

3 ROTOR DYNAMIC MODELLING OF TEST RIG INCLUDING SQUEEZE FILM DAMPERS

This section describes the test rig, it's components and all modelling parameters that were used for creating the rotor-bearing dynamics model. After that there is a description of rotor dynamic modelling. For modelling we are using RoBeDyn-toolbox in MATLAB. There is a description of RoBeDyn-toolbox and its features in this section. After that there is discussion about modular designing, discussion about demands and wishes for SFDs, defining the designing parameters for SFDs and designing progress step by step for SFDs. After that, there is shown how SFDs were modelled in SolidWorks and how the wanted features were modelled on them. Finally, there is description of used measuring equipment and data translation method.

3.1 Description of the test rig

The test rig consists from following components: electric motor, ROTEX shaft coupling, shaft, two magnetic bearing housings, two roller bearings, two bearing bushings, three weight discs and safety cage. Magnetic bearings are not used, because they are not relevant in this research. Instead of magnetic bearings, we are using roller bearings of test rig. For doing some measurements of test rig's vibrations, also acceleration sensors are needed in test rig. They will be attached on one of the bearing housings. The cut view from test rig can be seen in figure 5. More detailed information of test rigs components can be found on this section.

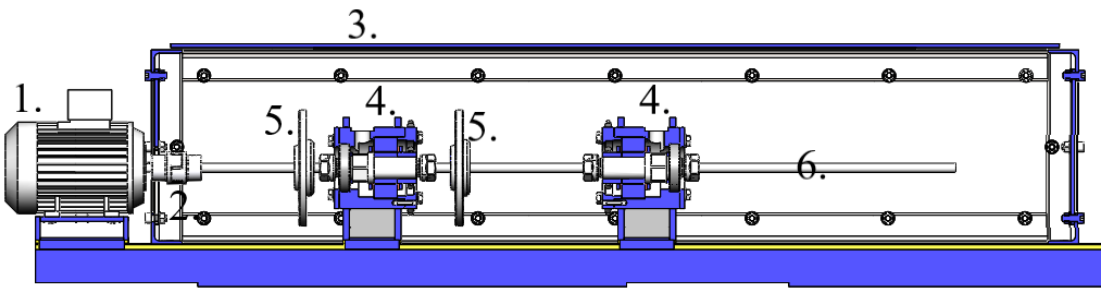

Figure 5. Cut view from the test rig.

Following components of test rig in figure 5 are shown in light grey color: 1. is the electric motor, 2. is ROTEX shaft coupling, 3. is the safety cage surrounding the rotor, 4. is bearing housing, 5. is weight disc and 6. is the shaft. Zoomed picture of the bearing housing near electric motor can be seen in figure 6.

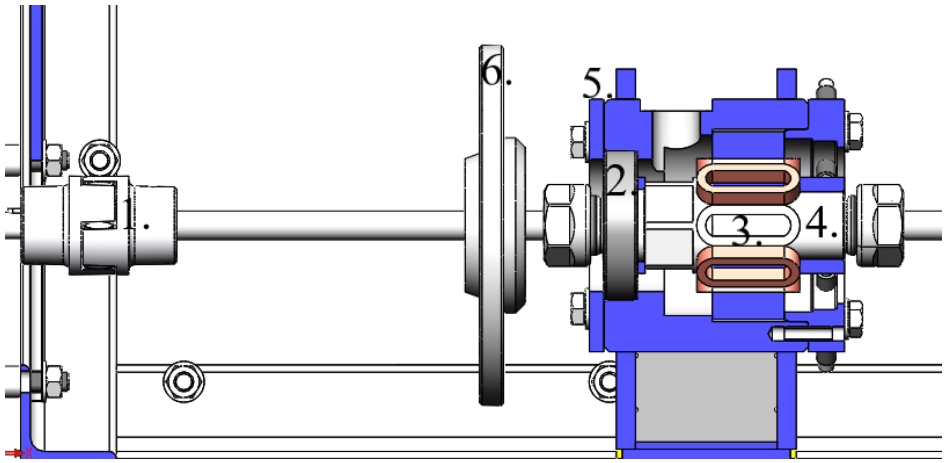

Figure 6. Zoom into the cut view of bearing housing. 1. is the ROTEX shaft coupling, 2. is a roller bearing, 3. is a magnetic bearing, 4. is a bearing bushing, 5. is the spot where acceleration sensor was attached and 6. is one of the weight discs.

3.1.1 Electric motor and ROTEX shaft coupling

Electronic motor is used for rotating the test rotor. The used electric motor is VEM motors Thurm K21R 63 K 2 H with 0.18 kW of power. The motor can be operated from 0 to 2765 revolutions per minute using three-phase inverter. The shaft is attached to the motor with ROTEX shaft coupling. ROTEX shaft coupling is designed, so that the motor can be easily attached and unattached from shaft, for example in maintenance purposes. The picture of electronic motor and ROTEX used in test rig can be seen in figure 7. (Sikanen 2019b & 2019c).

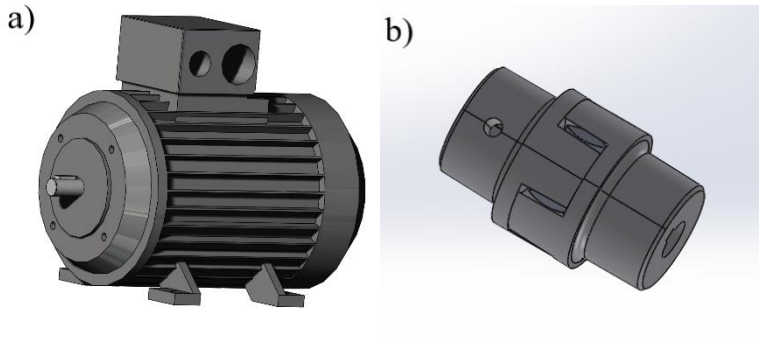

Figure 7. The electric motor and ROTEX of test rig. a) is motor and b) is ROTEX. (Sikanen 2019b).

The parameters for motor and ROTEX are shown in table 1.

Table 1. Parameters for motor and ROTEX. (VEM MOTOR 2017).

Motor:

Mass of axle, m	4.90 kg
Mass moment of inertia of axle in xx-direction, J_{xx}	0.00013 kg·m^2
Mass moment of inertia of axle in yy-direction, J_{yy}	0.00005 kg·m^2
Mass moment of inertia of axle in zz-direction, J_{zz}	0.00005 kg·m^2
Length of motor, L	0.178 m
Outer diameter of motor, d_{out}	0.118 m
Inner diameter of motor, d_{in}	0.00 m

ROTEX:

Mass of assembly, m	0.1345 kg
Mass moment of inertia in xx-direction, J_{xx}	$2.5780 \cdot 10^{-5}$ kg·m^2
Mass moment of inertia in yy-direction, J_{yy}	$2.5040 \cdot 10^{-5}$ kg·m^2
Mass moment of inertia in zz-direction, J_{zz}	$2.4860 \cdot 10^{-5}$ kg·m^2
Length, L	0.064 m
Outer diameter, d_{out}	0.041 m
Inner diameter, d_{in}	0.012 m

3.1.2 Magnetic bearings

Magnetic bearings are not used in this research, but they are attached in test rig. Magnetic bearings are located in the bearing housings, which also include the roller bearings. However, in this test rig, the magnetic bearings are not used in this research, but they might need to be in the rig for later researches. The magnetic bearings have outer diameter of 80 mm and the inner diameter is about 45 mm. The magnetic bearings are 30 mm thick. There are two magnetic bearings in the test rig. One of the magnetic bearings can be seen in figure 8.

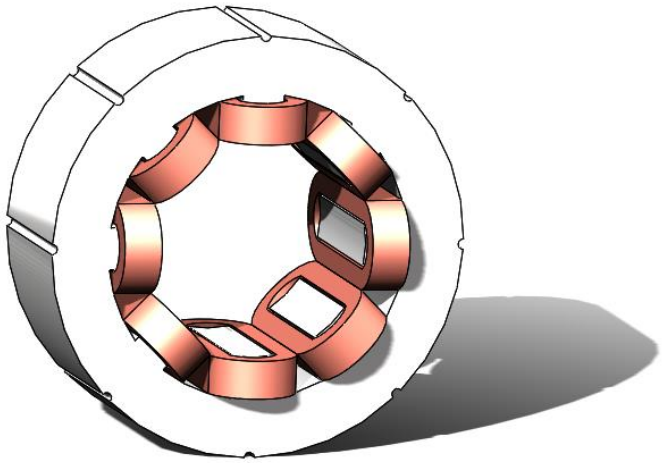

Figure 8. A magnetic bearing of test rig. (Sikanen 2019b).

3.1.3 Roller bearings and bushings

Roller bearings are used to reduce friction between rotor and stator. Bearing bushings are connecting the shaft and inner layer of bearings to each other. The roller bearings on the test rig are NSK 6007-ZZ. Diameter of these bearings is 62 mm and they are 14 mm thick. The inner diameter of the bearing is 35 mm. One bearing weights about 0.155 kg. Roller balls are 8.00 mm in diameter and there are 11 spherical roller elements in bearing. The roller bearings will be having SFDs around them, when this research is finished. There are two roller bearings in the test rig. Bearing bushings are connecting roller bearings into the shaft. A roller bearing and a bushing from test rig can be seen in figure 9. (Sikanen 2019b & 2019c, SKF 2019).

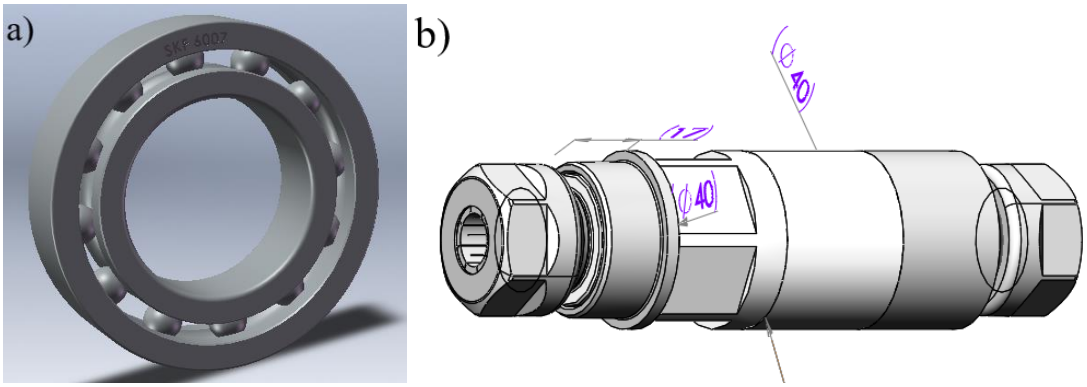

Figure 9. Roller bearing and bushing of test rig. a) is a roller bearing and b) is a bushing. (Sikanen 2019b).

The bearing's approximated stiffnesses and dampings are shown in table 2. Both bearings used in modelling are identical, so they have same numerical values for parameters.

Table 2. Bearing's approximated stiffnesses and dampings.

Bearings stiffness and damping:	
Stiffness in *Y*-direction (K_Y)	$2 \cdot 10^8$ N/m
Stiffness in *Z*-direction (K_Z)	$2 \cdot 10^8$ N/m
Damping in *Y*-direction (c_Y)	$1 \cdot 10^{-5}$ Ns/m
Damping in *Z*-direction (c_Z)	$1 \cdot 10^{-5}$ Ns/m

The parameters for bushings are shown in table 3.

Table 3. Bearing bushing parameters.

Bearing bushings:	
Mass of assembly, *m*	0.6996 kg
Mass moment of inertia in *xx*-direction, J_{xx}	0.00015204 kg·m^2
Mass moment of inertia in *yy*-direction, J_{yy}	0.00131352 kg·m^2
Mass moment of inertia in *zz*-direction, J_{zz}	0.00131353 kg·m^2
Length, *L*	0.127 m
Outer diameter, d_{out}	0.041 m
Inner diameter, d_{in}	0.012 m

3.1.4 Weight discs

The weight discs are in test rig to create unbalance in system. There are two weight discs in the test rotor, and they have diameter of 0.150 m and they weight about 1.69 kg each. The weight discs are 0.01 m thick. There are 24 of M6x10 holes where the unbalance mass can be added as bolts. The radius for those holes is 0.07 m. One DIN 933 M6 bolt weights about 0.00408 kg. This way the unbalance mass can be adjusted. The discs are made from DIN structural steel with elastic modulus 210 000 N/mm^2. A weight disc can be seen in figure 10. (Sikanen 2019b & 2019c).

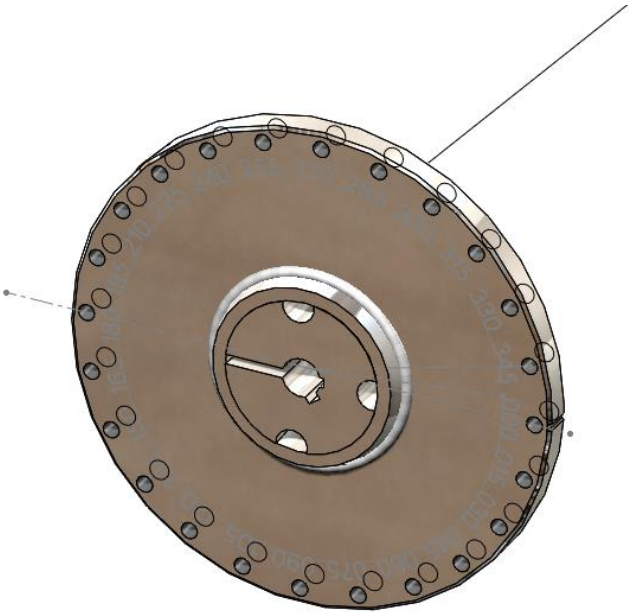

Figure 10. A weight disc of test rig. (Sikanen 2019b).

The parameters for weight discs are shown in table 4.

Table 4. Weight discs parameters.

Discs:	
Mass of one assembly, *m*	1.69 kg
Mass moment of inertia in *xx*-direction, J_{xx}	0.0038958 kg·m^2
Mass moment of inertia in *yy*-direction, J_{yy}	0.0019907 kg·m^2
Mass moment of inertia in *zz*-direction, J_{zz}	0.0019890 kg·m^2
Length, *L*	0.01 m

Table 4 continues. Weight discs parameters.

Discs:	
Outer diameter, d_{out}	0.150 m
Inner diameter, d_{in}	0.012 m

3.1.5 Safety cage

Safety cage is used for making the test rig safer. The safety cage will block any object that gets loose while operating the test rig and it prevents any external objects getting stuck into test rotor while it is operated, for example shirts sleeves or long hair. The safety cage is made from DIN structural S355 steel corner bars and there are invisible polycarbonate screens. The safety cage can be seen in figure 11. (Sikanen 2019b & 2019c).

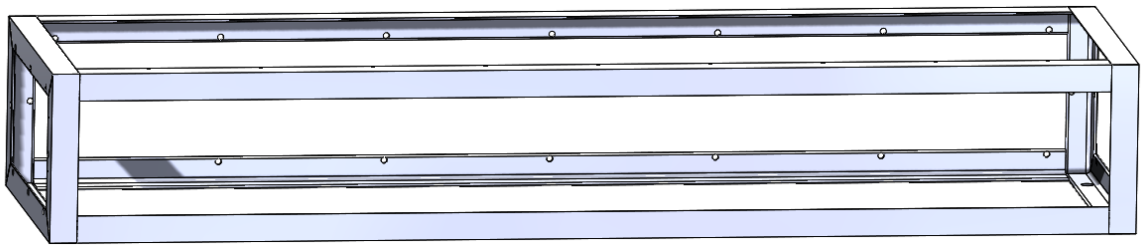

Figure 11. The safety cage of test rig. (Sikanen 2019b).

3.1.6 Shaft

The shaft is used to connect motor and the weight discs to each other and for power transmission. The shaft is 1000 mm long and 12 mm diameter DIN structural steel rod with elastic modulus of 210 000 N/mm^2. The shaft can be seen in figure 12. (Sikanen 2019b).

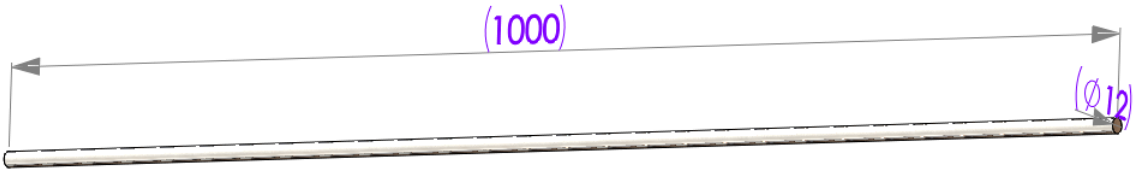

Figure 12. The shaft of test rig. (Sikanen 2019b).

3.1.7 Technical dimensions

Technical dimensions of test rig can be seen in figure 13.

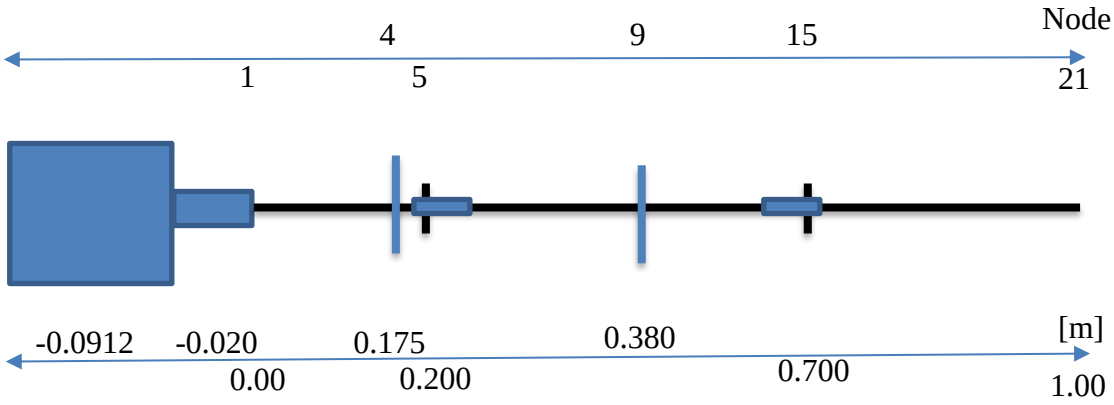

Figure 13. Technical dimensions of test rig. The upper line is showing location nodes for RoBeDyn-model and the lower line is showing the physical location of components mass centers in meters.

3.2 Rotor dynamic modelling

Rotor dynamic models can be built using Finite Element Method (FEM). However, general purpose FEM codes are not that good with rotor dynamics, because of the lack of gyroscopic effect in model (Genta 2005, p. 3). In this research we are using RoBeDyn-toolbox in MATLAB. RoBeDyn is a finite element-based tool for analyzing rotor dynamic systems. RoBeDyn is a tool designed for studying rotor dynamics with MATLAB. RoBeDyn-package can be used for modelling shafts, dampers, unbalanced masses, springs and bearings. The RoBeDyn can plot following graphs:

- Free-free modes of rotor system
- Campbell diagram
- Steady state responses
- Speeds of rotor instability
- Also, rotor's vibration mode shapes and deformed shapes can be plotted for pre-chosen rotation speed

The simplified researched system consists from two unbalance discs, two ball bearings, two SFDs, two bushings, one electric motor, one ROTEX shaft coupling and one shaft. Because of the two rotating discs, the system can be handled as multi degree of freedom-system (MDOF) (Goodwin 1989, p. 102-107). Figure 14 shows the simplified model of the test rig.

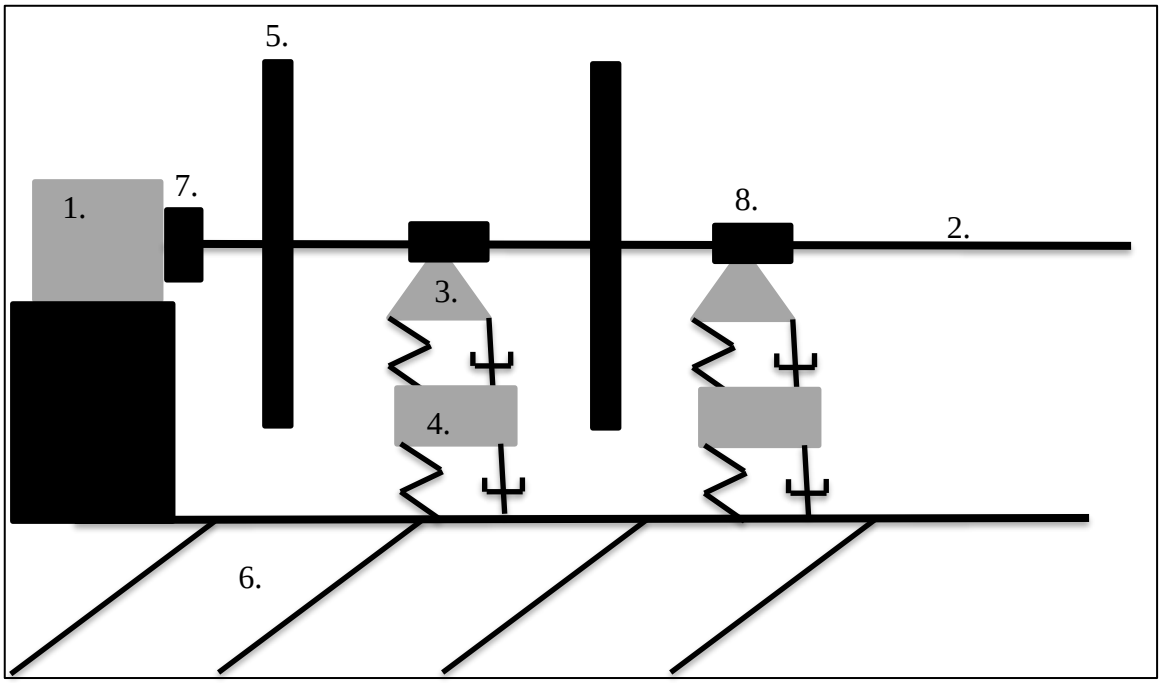

Figure 14. Simplified test rig. 1. is the electric motor, 2. is the shaft, 3. is the ball bearing with stiffness, 4. is squeeze film damper, 5. is an unbalance disc, 6. is fixed work bench, 7. is the ROTEX shaft coupling and 8. is a bushing.

Because the RoBeDyn is FE based tool, it relies in the elements and nodes (Burton 1994, p. 595-599). There are 20 elements in the model, which are 0.05 meters long. There are 23 nodes in model. 21 nodes are used to connect elements to each other, and two nodes are used for making supports for SFDs. Finite elements used in modelling are Timoshenko beam elements. Other elements used in modelling are rigid disc, spring and damper elements. There are eight point-masses in the system: motor, ROTEX-joint, two bearing bushings, two unbalance discs and two supports. The shaft is modelled with 12 mm diameter. The picture of described system in RoBeDyn can be seen in figure 15.

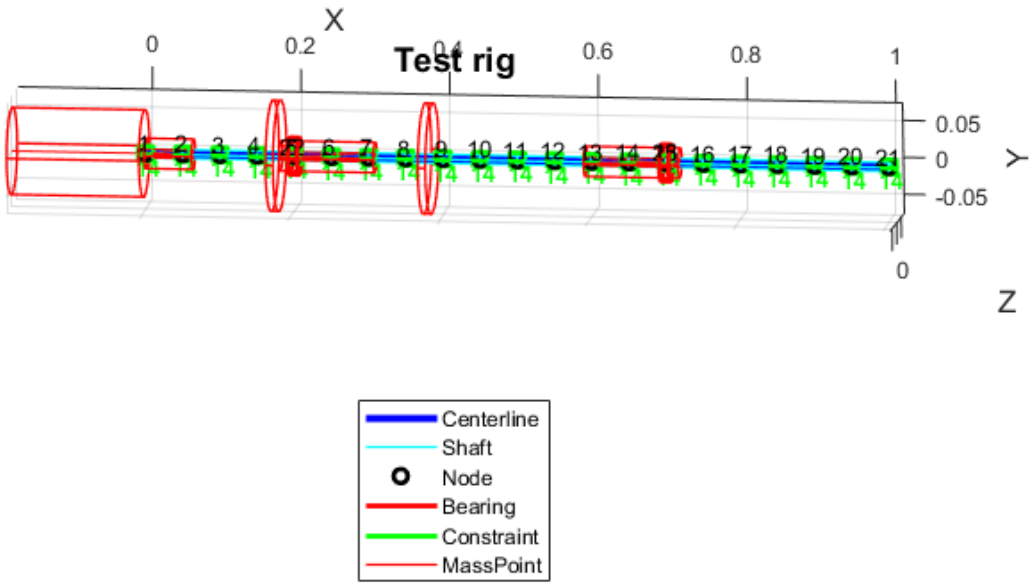

Figure 15. Described RoBeDyn-model. *X*, *Y* and *Z* are showing in which way the coordinate axis is. Units for all axis are marked as meters.

All nodes have six degrees of freedom. The possible degrees of freedom are displacement in *X*-, *Y*- and *Z*-direction and rotations around *X*-, *Y*- and *Z*-axis (Dankowicz 2005, p. 368-376). Constraints are reducing the number of degrees of freedom, which means that the nodes cannot move in constrained way (Pfeiffer 2008, p. 6-8). Nodes on shaft (1-21) have set constraints so that they cannot move in *X*-direction or rotate in *X*-direction. Support nodes 22 and 23 have constraints so they cannot move in *X*-direction or rotate in *X*-, *Y*- or *Z*-direction (Amirouche 2006, p. 321-322). Material properties used in modelling are listed in table 5.

Table 5. Material properties used in modelling.

Density of material, *rho*	7800 kg/m^3
Elastic modulus, *E*	$2.1 \cdot 10^{11}$ Pa
Poisson's ratio, *v*	0.3
shear correction factor, k_s	0.8864

Mass point offsets for weight discs, ROTEX, bushings, motor and supports are mentioned in table 6. Mass point offset means the axial distance between the center of a mass of a component and between node the component is located.

Table 6. Modelling parameters for mass point offsets.

Component	*h*, mass point offset [m]
Disc 1	0.025
Disc 2	-0.01
ROTEX	0.032
Bushing 1	0.04495
Bushing 2	-0.04495
Motor	-0.0912
SFD 1	0
SFD 2	0

The parameters used in table 6 were used for adjusting mass points in right locations in RoBeDyn-model.

The parameters of unbalanced masses in discs can be seen in table 7.

Table 7. Unbalanced masses parameters.

Unbalanced masses:	
Location nodes:	4 and 9
Value for node 4 unbalance [kg·m]	$7.140 \cdot 10^{-5}$
Value for node 9 unbalance [kg·m]	0
Angle for unbalance at node 4 [rad]	0
Angle for unbalance at node 9 [rad]	0

The parameters in table 7 are based into the inserted masses into the weight discs. The amount of mass and the angle of the mass can be adjusted in discs by moving or removing weights from the discs.

There are two bearings and two dampers in model. Bearings are attached into test rotor. SFDs are attached to the bearings and SFDs are also attached as fixed into ground. Bearings and dampers have stiffness and damping modelled on them. Table 8 shows the parameters for bearings and SFDs.

Table 8. Parameters for springs and dampers in bearings and SFDs.

Bearings:	
Start nodes:	5, 15
End nodes:	22, 23
Direction:	*Y* and *Z*
Start nodes:	22, 23
End nodes:	0 (fixed), 0 (fixed)
Direction:	*Y* and *Z*
Stiffness before adjusting:	0, 0
Damping before adjusting:	0, 0

Figure 16 shows how the springs and dampers are in RoBeDyn-model.

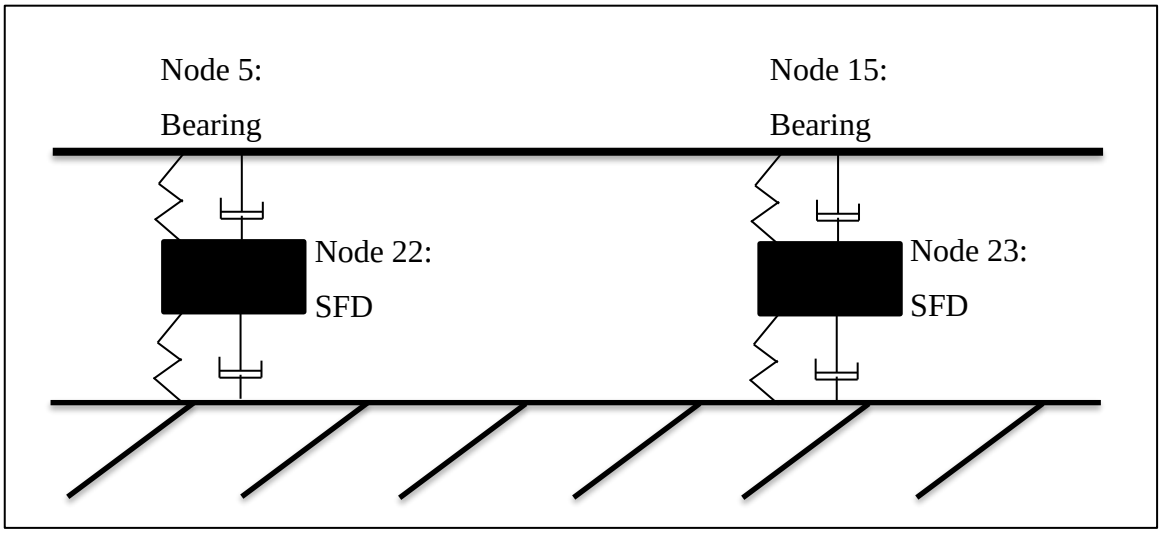

Figure 16. The location of springs and dampers in RoBeDyn-model.

The most important codes from made RoBeDyn-model are at Appendix I and Appendix II.

3.3 Designing of SFDs

Modular design is design theory and practice that divides the assembly into smaller subassemblies. The subassemblies can be changed, and the properties of assembly can be modified with that (Stone 1997). On this research, we are interested about adding a modular damping unit into the bearing houses. From figure 17, we can see the area where SFDs will be added.

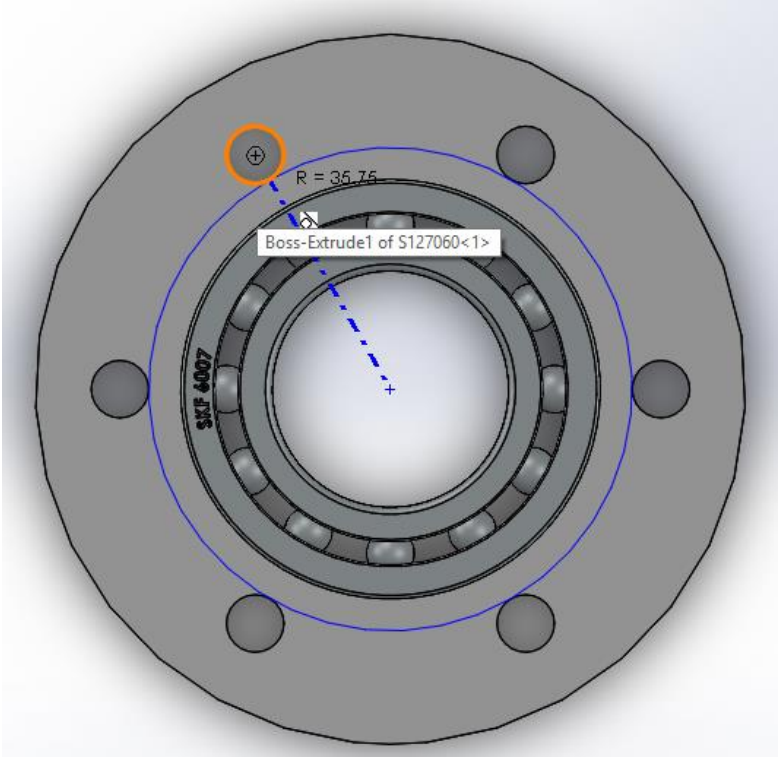

Figure 17. Area for SFD. The outer limit is marked on blue color. The components on this subassembly are the bearing and the lid of bearing house.

We can see from the figure 17, that there is not very much space between the bearings outer layer and between the bolt holes in the lid. The bearing has 31 mm radius and the bolts are from 35.75 mm from the center point of the lids center, so there is 4.75 mm space for the damper. The bearing has a bushing in it, so there is no extra space for damper. Figure 18 shows the situation.

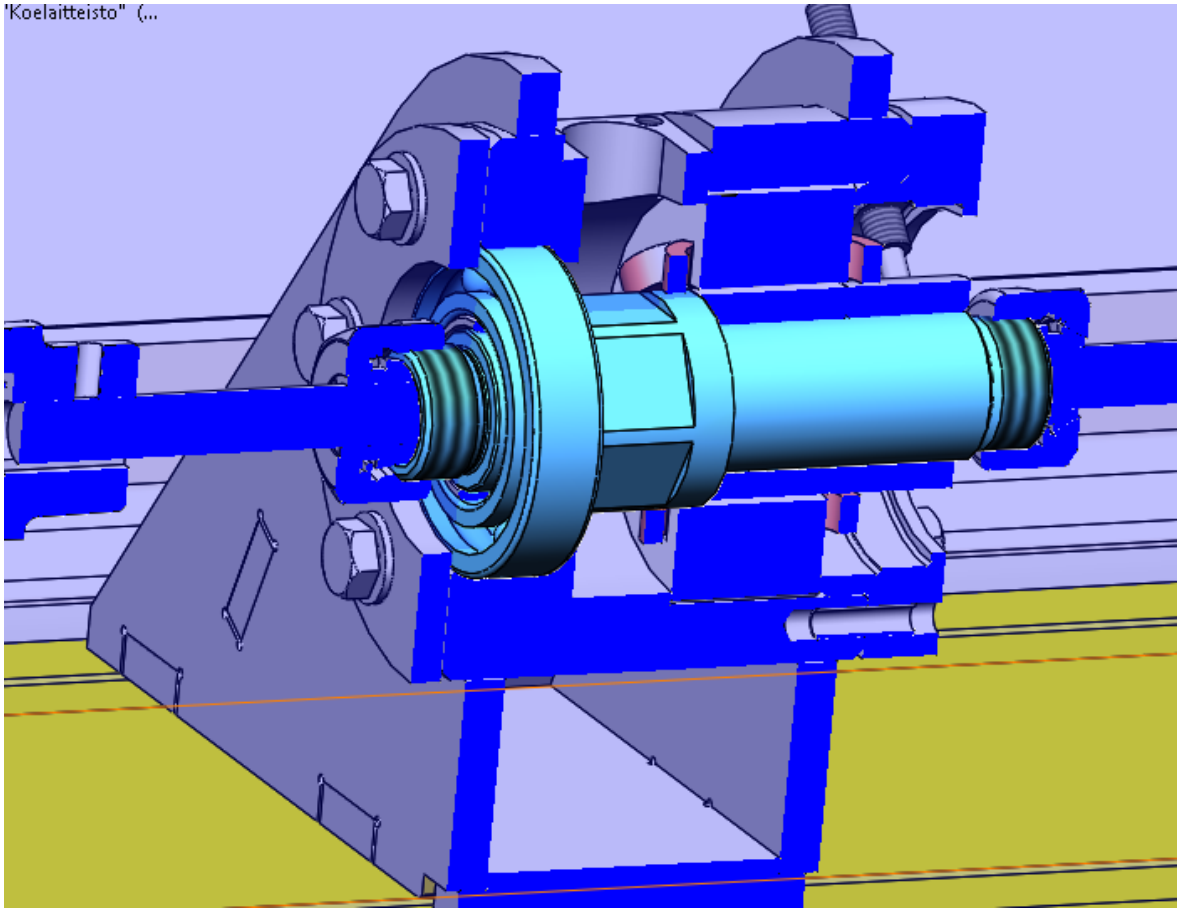

Figure 18. Section view from bearing house. The bushing and bearing are shown in light blue color.

There were some demands for designing SFDs. Designed SFDs need to have same dynamic behavior in *Y*- and *Z*-direction. This means that they need to have same value for damping in *Y*- and *Z*-direction and for stiffness in *Y*- and *Z*-direction. Designed SFD needs to be a modular unit, so it is easy to assemble and dissemble from test rig. Because the bearings outer diameter is 62 mm, the inner diameter for SFD needs to be 62 mm. Because bearings are 14 mm thick, SFD can be 14 mm thick maximum. SFDs need to lower vibrations in test rig. This can be achieved by designing SFD with optimal stiffness-damping ratio that dramatically will decrease vibrations in test rotor. There were also some wishes according the design. Designed SFDs need to fit in original bearing housing. This means that the maximum outer diameter for SFD is 71.5 mm. Design parameters for SFDs are collected in table 9.

Table 9. Parameters for designing SFDs

SFDs:

Direction:	*Y* and *Z*
Stiffness *Y*-direction:	$2 \cdot 10^5$ … $4 \cdot 10^5$ N/m
Stiffness *Z*-direction:	$2 \cdot 10^5$ … $4 \cdot 10^5$ N/m
Damping *Y*-direction:	2000 Ns/m
Damping *Z*-direction:	2000 Ns/m
Max outer diameter:	71.5 mm
Inner diameter:	62 mm
Thickness:	14 mm

The first step to start modelling in SolidWorks was to create a ring-shaped object with inner diameter of 62 mm, outer diameter of 71.5 mm and with thickness of 14 mm. There were no oil grooves yet, this test was done for finding out suitable stiffness for SFDs. However, static simulations in SolidWorks showed that stiffness of this kind of SFDs is too high.

Next step was to design SFD with smaller outer diameter, while keeping inner diameter and thickness on suitable values. This time the outer diameter for SFD was 68 mm. There were no oil grooves in model this time either. This time static simulations in SolidWorks showed that SFD with these dimensions have stiffness that is moderately close $2 \cdot 10^5$ - $4 \cdot 10^5$ N/m in *Y*- and *Z*-direction, but values were not high enough.

For adjusting stiffness higher, there need to be parts that act like springs in SFD. A spring in SFD is curve shaped part, what is separated from other springs with oil groove between them. The more there are these spring segments in SFD, the higher stiffness SFD will be having. By taking account, that SFD's stiffness need to be same in *Y*- and *Z*-direction, number of springs was increased by two for each design model. Damping was not taken account at this point yet, but it can be adjusted by changing the thickness of oil film inside SFD. The result from this designing was SFDs with two-, four-, six- and eight-spring model. SFDVER9 has two springs on it, SFDVER10 has four springs on it, SFDVER11 has six springs on it and SFDVER12 has eight springs on it. The inner and outer diameter, thickness and thickness of springs on these models were same. These all designed models were small

enough to fit in original bearing housing too. Example figure of modelled SFD can be seen in figure 19.

Figure 19. Example of modelled SFD. This SFD has eight springs on it.

3.4 Done measurements

Measurements were done with 1D-sensor, amplifier and with a mixed signal oscilloscope. Piezo sensor creates a small voltage, when the sensor changes dimensions (Beckwith, Buck & Marangoni 1982, p. 106-108). Used 1D sensors had a magnet on them so they could be fastened into the test rig without any other joint. The vibration sensor was attached into the bearing house nearby motor, so that it was measuring horizontal acceleration. An 1D-sensor used in measurements can be seen in figure 20.

Figure 20. 1D-sensor that was used in measurements.

The voltages created by the 1D-sensors are too small to be recognized in the oscilloscope, so the signal needs to be amplified first. The amplifier used in measurements was a Brüel & Kjær Charge Amplifier Type 2635. With this amplifier the voltage of input signal was amplified to the needed voltage for oscilloscope and some of the wavelengths were filtered out from the signal. Picture of the amplifier can be seen in figure 21.

Figure 21. Brüel & Kjær Charge Amplifier Type 2635.

Amplifier was connected to the Tektronix 5. series mixed signals oscilloscope. The oscilloscope was used to record, display and for scaling measured signals. The used oscilloscope has an option to save measured signals as csv-files to the oscilloscope's memory or to the external database, such as USB-stick. The oscilloscope had four different channels for four different measurement equipment's, but only one channel was needed in measurements because there was only one 1D-sensors being used. The figure of used oscilloscope can be seen in figure 22.

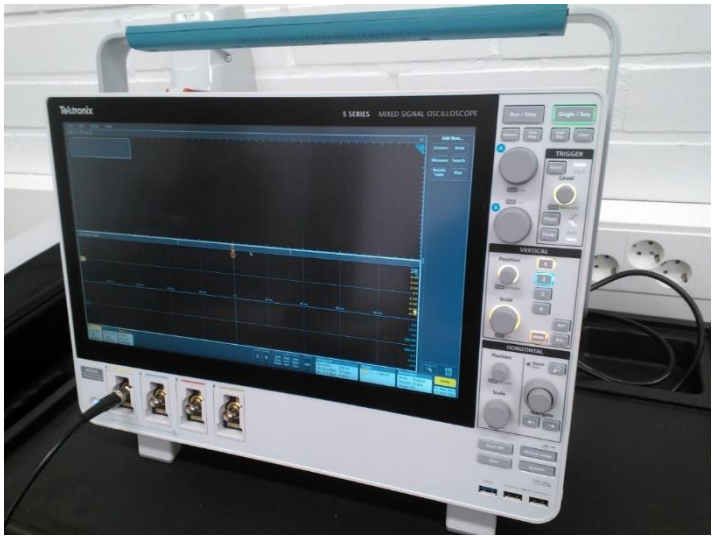

Figure 22. Oscilloscope used in measurements.

The saved time domain data from oscilloscope needed to be modified, so the measured response for different frequencies could be plotted. The measured signal was modified with fast Fourier transform to achieve that plot. This transformation protocol turned the original signal to the needed frequency-amplitude-plot. The FFT-conversion fitted the data in reasonable scale of frequency, by thinking that motor in test rig is only capable to reach 50 Hz and plotted the response in system as a function of frequency. This was used for finding out the resonance frequencies in the system with done measurements. The example of unmodified and modified signal can be seen in figure 23.

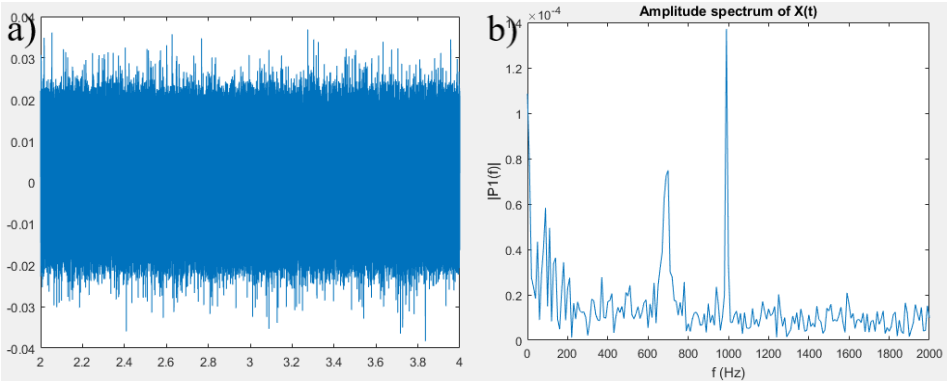

Figure 23. Measured signal and modified signal. a) is the measured unmodified signal and b) the fast Fourier transformed signal.

4 RESULTS

The results from literature, from simulation models and from measurements are collected on this section. First there are some most important findings from rotor dynamics literature and from SFD-theory. Then there are results from the test rigs RoBeDyn-model such like Campbell diagram and unbalance response. Then there are results from SolidWorks and from designing of SFDs dimensions. Finally, there are results from the done measurements, which are used for verifying the RoBeDyn-model.

4.1 Results from literature review

Integral squeeze film dampers were mentioned to be assembled around the bearings and having no need for oil pump to operate (Waukesha Bearings 2019b). This gave and inspiration to design an ISFDs to the test rig. As a result, the modelled SFD will be fitting into the bearing house with original bearings. This solution is also good by taking accord modular design. The SFDs will be easy to assemble, replace or be changed to the other module.

4.2 RoBeDyn results

These results were gained from the done numerical model of test rig. The model is called as RoBeDyn-model. Important results about numerical models' dynamical behavior are forward and backward whirling modes as a function of rotation speed, vibration amplitudes as a function of rotation speed and different whirling modes while system is resonating. Results were gained from the Campbell diagram, from the unbalance response plot and from numerical models' whirling mode analysis. Because, the electric motor can only operate at 0-3000 RPM, the results are gained using 3000 RPM as maximum.

4.2.1 Campbell diagram

Campbell diagram shows the forward and backward whirling modes of system a function of rotation speed (Genta 2005, p. 9). The results were gained without SFDs. A Campbell diagram of the numerical model can be seen in figure 24.

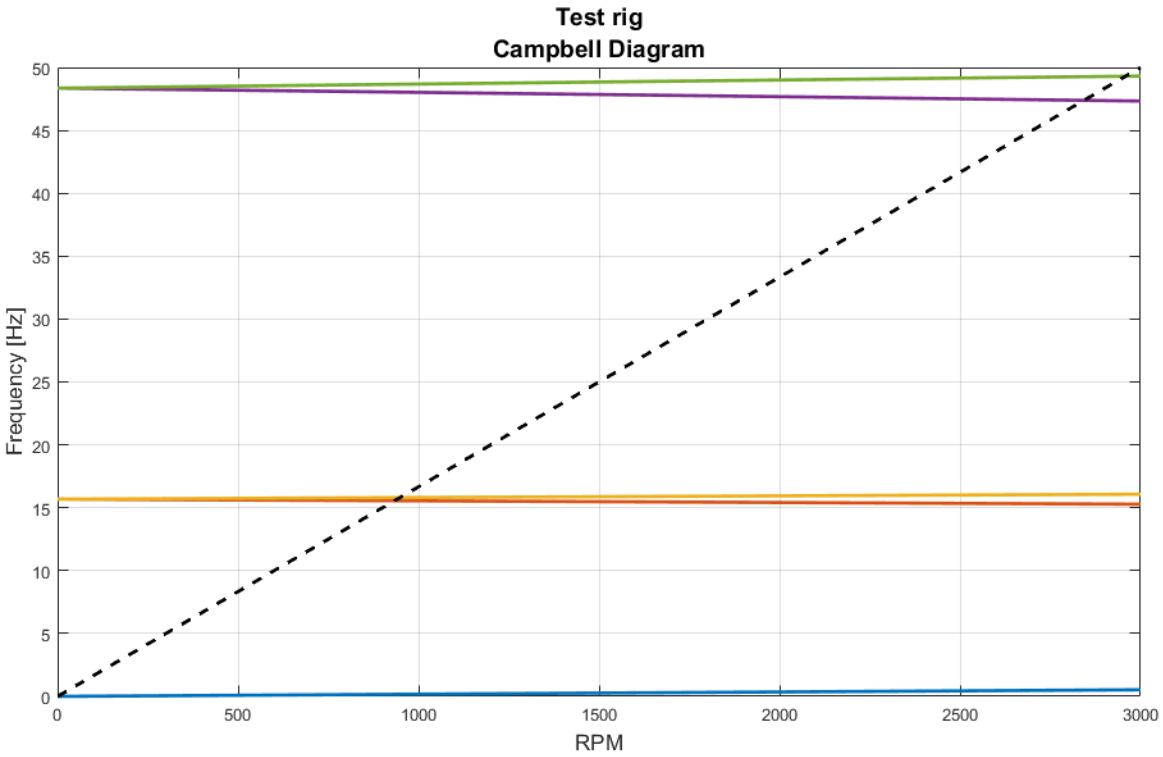

Figure 24. Campbell diagram of test rig from RoBeDyn-model. We can see that the system has forward whirling modes at 0, 948 and 2958 and backward whirling modes at 933 and 2843 RPM. *X*-axis is rotation speed in unit of RPM and *Y*-axis is frequency in unit of Hz.

4.2.2 Unbalance response

Unbalance response plot from model without SFDs, shows the vibration amplitude of system as a function of rotation speed (Genta 2005, p. 23-26). The results were gained without SFDs. An unbalance response plot from the numerical model can be seen in figure 25. The amount of unbalance in discs is only meant for analyzing the system in RoBeDyn-model and the used unbalance might be too big for the real-life test rig.

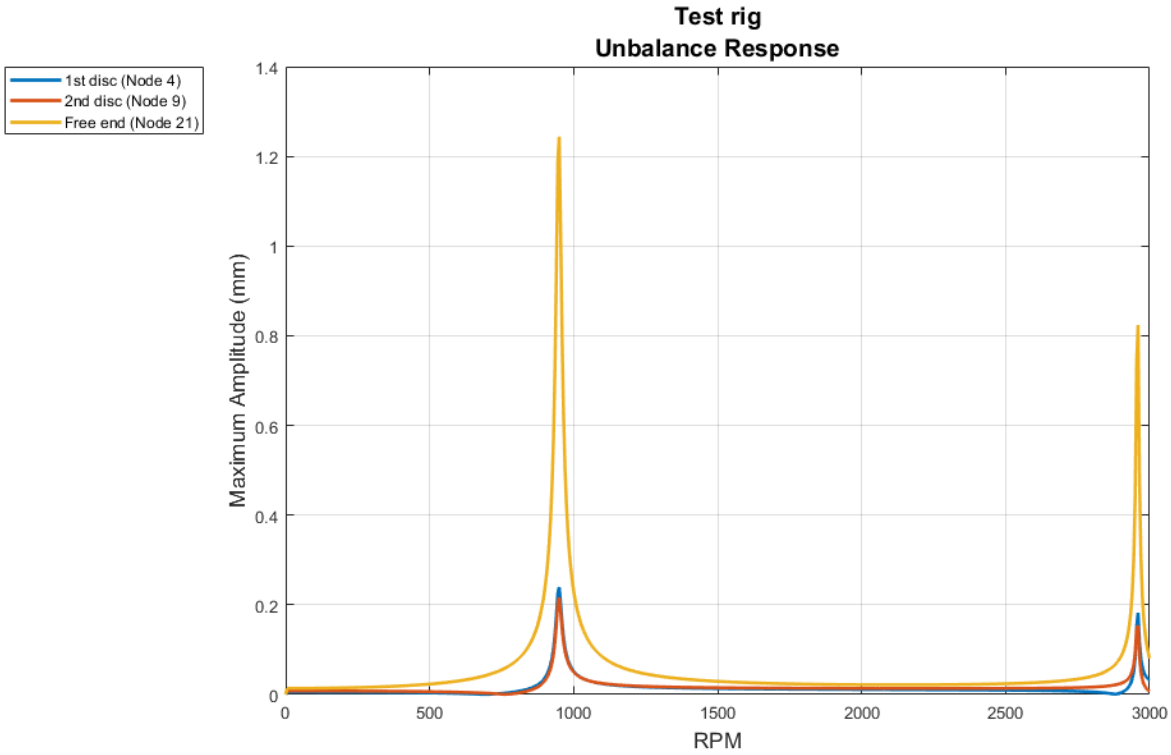

Figure 25. Unbalance response plot of test rig from numerical model.

We can see from figure 25 that the system is resonating strongly at 950 RPM and at 2960 RPM. Figure 25 shows that the maximum amplitude is at shaft free end and it is 1.244 mm. In figure 25, node 4 is marked as yellow and it is locating where the first weight disc, starting from the motor, is locating. Node 9 is marked as orange and it is locating where the second weight disc, starting from the motor, is locating. Node 21 is marked as blue and it is locating where shaft free end is locating. In figure 25, *X*-axis is rotation speed in unit of RPM and *Y*-axis is amplitude of vibration in unit of mm.

4.2.3 Whirling modes

Whirling modes are showing the mode response to specific pre-chosen frequency. We have chosen frequencies that the system is resonating as pre-chosen frequencies. There can be forward whirling, backward whirling or mixed whirling, which is mix of forward and backward whirling. Figure 26 is showing whirling modes from test rig gained by RoBeDyn-model at 950 RPM. There are no SFDs in model.

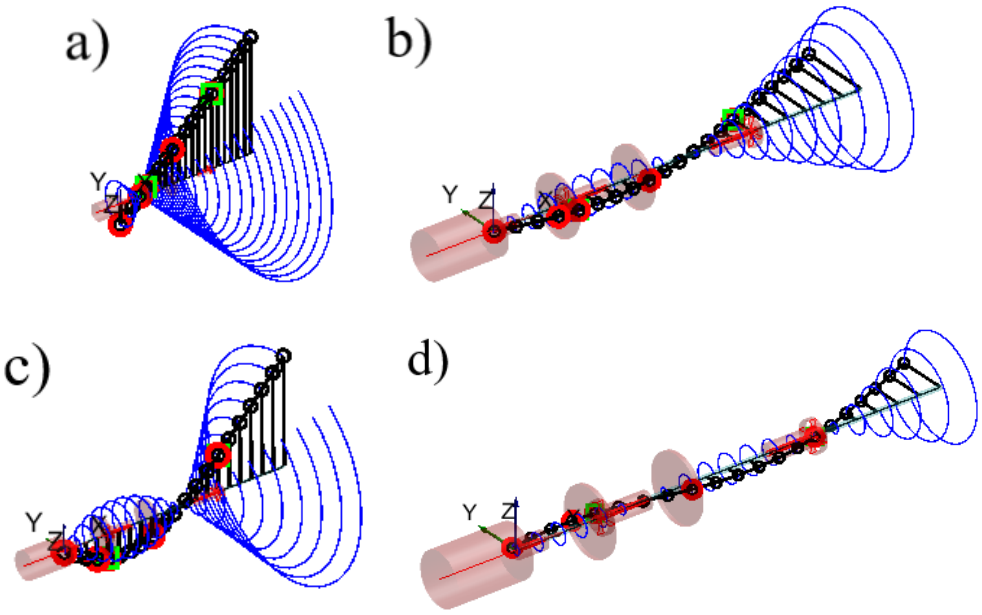

Figure 26. Whirling modes at 950 RPM. a) is the first mode, b) is the second mode, c) is the third mode and d) is the fourth mode.

With 950 RPM, the first mode is at 0.1671 Hz, with 0.000% damping ratio and that is a forward whirling mode. The second mode is at 15.55 Hz, with 0.98% damping ratio and that is a backward whirling mode. The third mode is at 15.81 Hz, with 0.98% damping ratio and that is a forward whirling mode. The fourth mode is at 48.04 Hz, with 0.149% damping ratio and that is backward whirling mode.

Figure 27 is showing whirling modes from test rig gained by RoBeDyn-model at 2960 RPM. There are no SFDs in model.

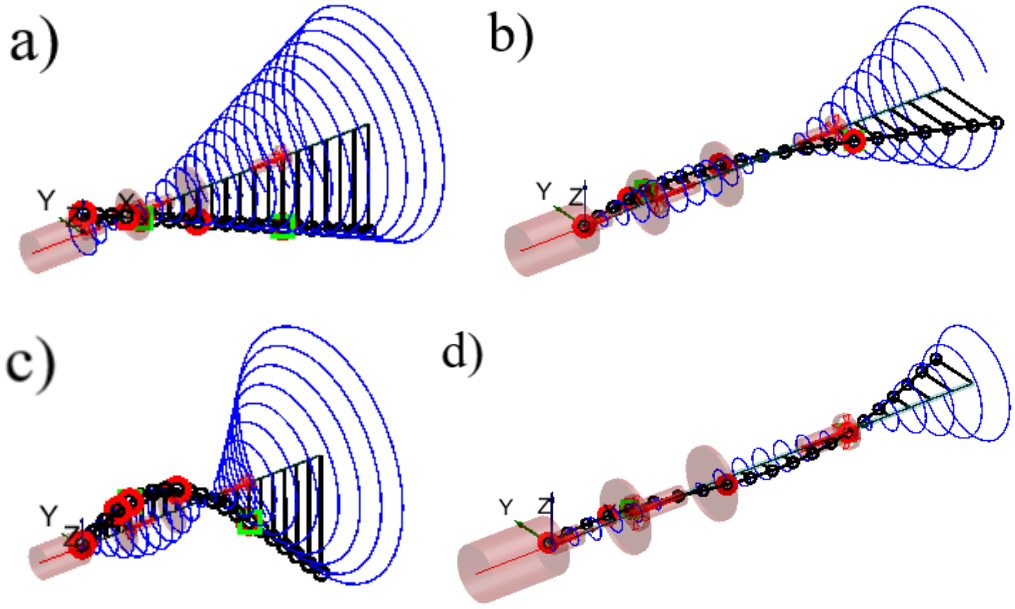

Figure 27. Whirling modes at 2960 RPM. a) is the first mode, b) is the second mode, c) is the third mode and d) is the fourth mode.

With 2960 RPM, the first mode is at 0.5202 Hz, with 0.000% damping ratio and that is a forward whirling mode. The second mode is at 15.29 Hz, with 0.979% damping ratio and that is a backward whirling mode. The third mode is at 16.07 Hz, with 0.98% damping ratio and that is a forward whirling mode. The fourth mode is at 47.35 Hz, with 0.149% damping ratio and that is backward whirling mode.

4.3 SFD modelling results

This section shows the most important results and findings from modelling SFDs and by using SolidWorks a modelling tool of SFDs. By using static analysis in SolidWorks, we were able to define the stiffness of designed SFDs. By using suitable equation about designed SFDs damping, we were able to define damping for designed SFDs. These gained values were used for researching SFDs behavior in RoBeDyn-model. This section also shows which of the design models of SFDs was selected as a final design version and why.

4.3.1 SFD damping

The damping's of SFDs were gained by using the equation 5. We can think that the SFDs are made from two separate oil films with different radiuses. Table 10 is showing the calculation of damping for SFDs. Only changing variable is the thickness of oil film (c_c).

Table 10. SFD damping calculation.

Test	η (Pa·s)	R_1 (m)	R_2 (m)	L (m)	c_c (m)	C_{SFD} (Ns/m)
1	$142.2 \cdot 10^{-3}$	$32.0 \cdot 10^{-3}$	$33.0 \cdot 10^{-3}$	$14.0 \cdot 10^{-3}$	$0.05 \cdot 10^{-3}$	$3.1872 \cdot 10^{5}$
2	$142.2 \cdot 10^{-3}$	$32.0 \cdot 10^{-3}$	$33.0 \cdot 10^{-3}$	$14.0 \cdot 10^{-3}$	$0.10 \cdot 10^{-3}$	$3.9840 \cdot 10^{4}$
3	$142.2 \cdot 10^{-3}$	$32.0 \cdot 10^{-3}$	$33.0 \cdot 10^{-3}$	$14.0 \cdot 10^{-3}$	$0.20 \cdot 10^{-3}$	$4.9800 \cdot 10^{3}$
4	$\mathbf{142.2 \cdot 10^{-3}}$	$\mathbf{32.0 \cdot 10^{-3}}$	$\mathbf{33.0 \cdot 10^{-3}}$	$\mathbf{14.0 \cdot 10^{-3}}$	$\mathbf{0.27 \cdot 10^{-3}}$	$\mathbf{2.0241 \cdot 10^{3}}$

From table 10, we can see that the 0.27 mm thick oil films in SFD gives damping that is in wanted area, because it has the damping very close to the wanted 2000 Ns/m.

4.3.2 SFD stiffness

Stiffnesses of SFDs were gained by doing static simulations in SolidWorks. The outer layer of SFD was set as fixed. Forces were set in *Y*- or *Z*-direction to the inner layer of SFD to make it deform. By knowing displacement and force that caused the displacement, we will be able to calculate stiffness of SFD. The SolidWorks ran the static simulations and gave out as a result, the displacements in model caused by the applied forces. Gained maximum displacement from each simulation was used for defining the stiffness of SFD. Simulation parameters for calculating the stiffnesses for SFDs are collected in the table 11.

Table 11. SFD stiffness calculating parameters.

Model	F_Y (N)	U_Y (mm)	K_Y (N/m)	F_Z (N)	U_Z (mm)	K_Z (N/m)
SFDVER9	10	1.9380	$5.2 \cdot 10^{3}$	10	0.4924	$20.3 \cdot 10^{3}$
SFDVER10	**100**	**0.2572**	$\mathbf{388.8 \cdot 10^{3}}$	**100**	**0.2572**	$\mathbf{388.8 \cdot 10^{3}}$
SFDVER11	100	0.0283	$3528.6 \cdot 10^{3}$	100	0.0306	$3265.8 \cdot 10^{3}$
SFDVER12	100	0.0071	$14172.3 \cdot 10^{3}$	100	0.0070	$14192.4 \cdot 10^{3}$

We can see from the table 11, that the SFDVER10, what has four springs on it, is giving the stiffness that is in wanted range $2 \cdot 10^{5}$ – $4 \cdot 10^{5}$ N/m. Also, the SFDVER10s stiffness in *Y*- and *Z*-directions are very close to each other. That means designed SFD is behaving in a same way in *Y*- and *Z*-direction. The example figure of static simulation in SolidWorks can be seen in figure 28.

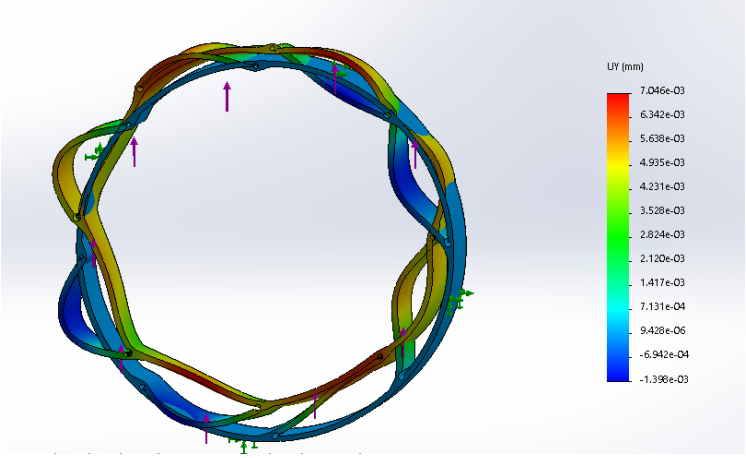

Figure 28. Example static simulation done in SolidWorks for calculating stiffnesses for SFDs. The deformations are not in right scale, so they are unrealistic. The maximum displacement in this simulation was about 0.0070 mm. The real system would not deform this way, because SFD's components are deforming so that they penetrate each other. This is caused by too big scaling factor for deformations.

4.3.3 Selecting of the suitable SFD

The modelling parameters, stiffnesses and damping for designed SFD are collected in table 12.

Table 12. SFD modelling parameters.

Feature	Parameter	Unit
Inner diameter (d_{in})	62	mm
Outer diameter (d_{out})	68	mm
Length (L)	14	mm
Amount of springs (n)	4	-
Radius of first oil film (R_1)	32	mm
Radius of second oil film (R_2)	33	mm
Thickness of oil films (c_c)	0.1	mm
Damping (C_{SFD})	2024	Ns/m
Stiffness in Y-direction (k_{SFDy})	$388.8 \cdot 10^3$	N/m
Stiffness in Z-direction (k_{SFDz})	$388.8 \cdot 10^3$	N/m

The designed SFDs were tested in RoBeDyn-model with parameters listed in table 13 and their maximum amplitudes in different location were listed also to table 13. Node 4 is the location of first weight disc, Node 9 is the location of second weight disc and Node 21 is the shafts free end.

Table 13. Amplitudes with designed SFDs.

Model	C_{SFD} (Ns/m)	k_{SFDy} (N/mm)	k_{SFDz} (N/mm)	Max amplitude Node 4 (mm)	Max amplitude Node 9 (mm)	Max amplitude Node 21 (mm)
SFDVER9	$2.0241 \cdot 10^3$	5.2	20.3	0.01174	0.05033	0.1682
SFDVER10	$2.0241 \cdot 10^3$	388.8	388.8	0.01016	0.07293	0.2110
SFDVER11	$2.0241 \cdot 10^3$	3528.6	3265.8	0.1137	1.1170	3.512
SFDVER12	$2.0241 \cdot 10^3$	14172.3	14192.4	0.2768	2.057	6.634

In figure 29 we can see the unbalance responses from designed SFDs listed on table 13.

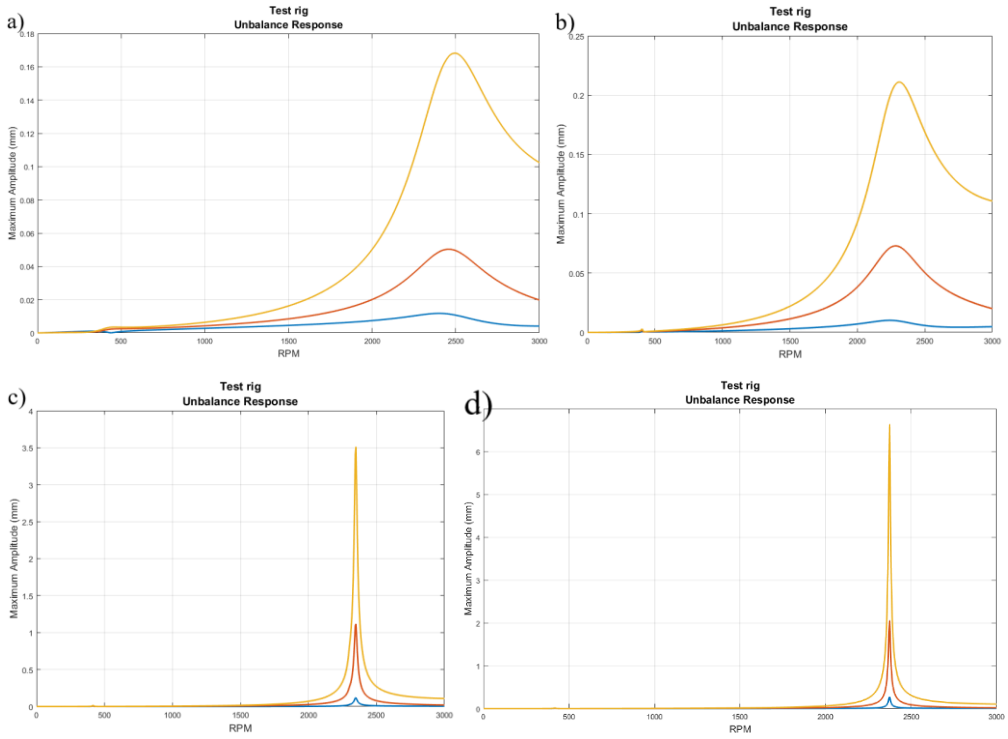

Figure 29. Unbalance response-plots with different SFDs. a) is the SFDVER9, b) is the SFDVER10, c) is the SFDVER 11 and d) the is SFDVER12.

In figure 29, node 4 is marked as yellow and it is locating where the first weight disc, starting from the motor, is locating. Node 9 is marked as orange and it is locating where the second weight disc, starting from the motor, is locating. Node 21 is marked as blue and it is locating where shaft free end is locating. *X*-axis are rotation speed in unit of RPM and *Y*-axis are amplitude of vibration in unit of mm.

In figure 30 we can see the Campbell diagrams from designed SFDs listed on table 13.

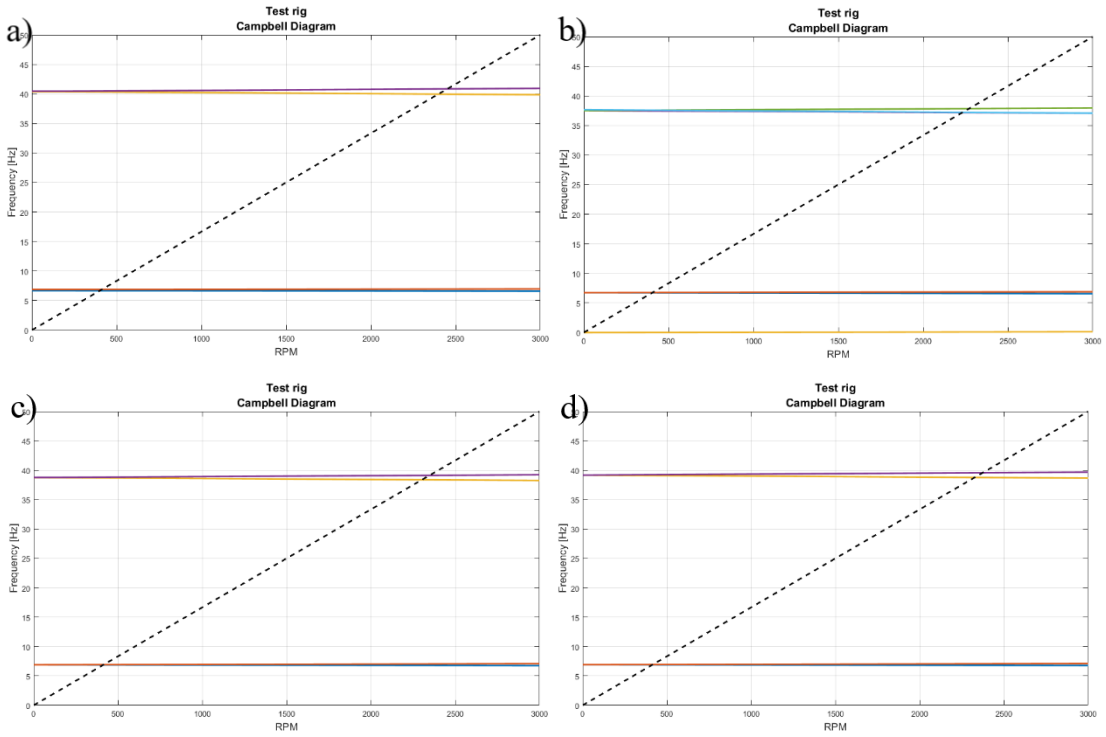

Figure 30. Campbell diagrams with different SFDs. a) the is SFDVER9, b) is the SFDVER10, c) is the SFDVER 11 and d) is the SFDVER12. *X*-axis are rotation speeds in unit of RPM and *Y*-axis are frequency of vibration in unit of Hz.

4.4 Results from the measurements

The results from done measurements are shown in this part. The measurements were done with one 1D acceleration sensor for stationary rotor. 1D sensor was attached in both measurements in exactly the same point. The point where sensor located was in the top of the first bearing house starting from the electric motor. Measurements were done by hitting the bearing house with rubber hammer to create an impulse in system. Systems response to impulse was measured with 1D sensor, amplified, and graphically displayed. Measurements

included two different measurements. The other was done for rotor that did not have motor attached into it. This measurement was called “only shaft”-measurement. On this measurement, there were no dampers in rig. Figure 31 shows the amplitude spectrum of signal to 2000 Hz and the zoom of amplitude spectrum of 0 – 110 Hz.

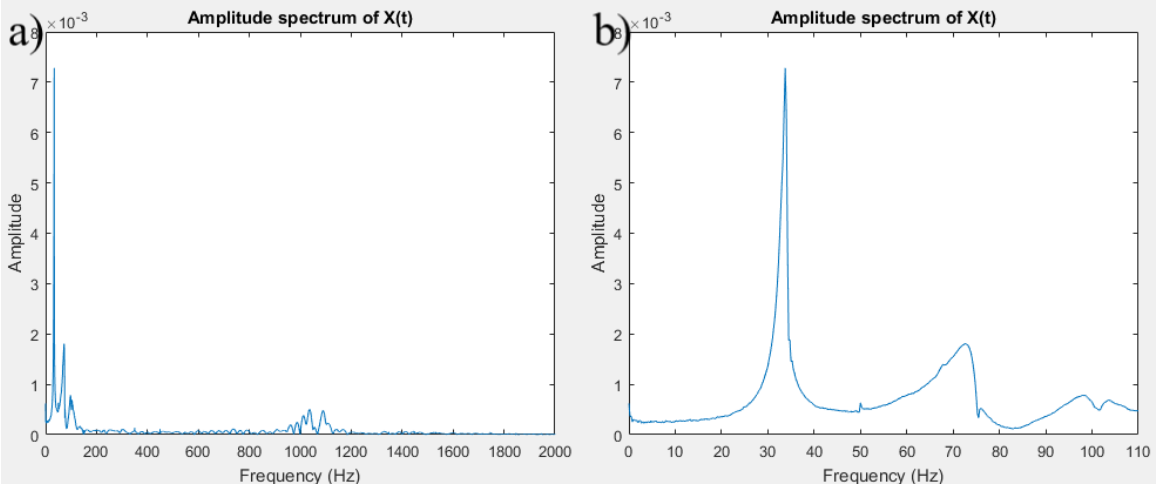

Figure 31. Measured amplitude spectrum from shaft only- measurement and it’s zoom. a) is the amplitude spectrum to 2000 Hz and b) is a zoom of 0 – 110 Hz. We can see that the system is resonating at about 34 Hz, 72 Hz, 100 Hz, 1037 Hz and 1090 Hz. *X*-axis are frequency in unit of Hz and *Y*-axis are amplitude of vibration in unit of m.

The other measurement was done for test rotor that had the electric motor attached into it. This measurement was called “with motor”-measurement. On this measurement, there were no dampers in rig. Figure 32 shows the amplitude spectrum of signal to 2000 Hz and the zoom of amplitude spectrum of 0 – 110 Hz.

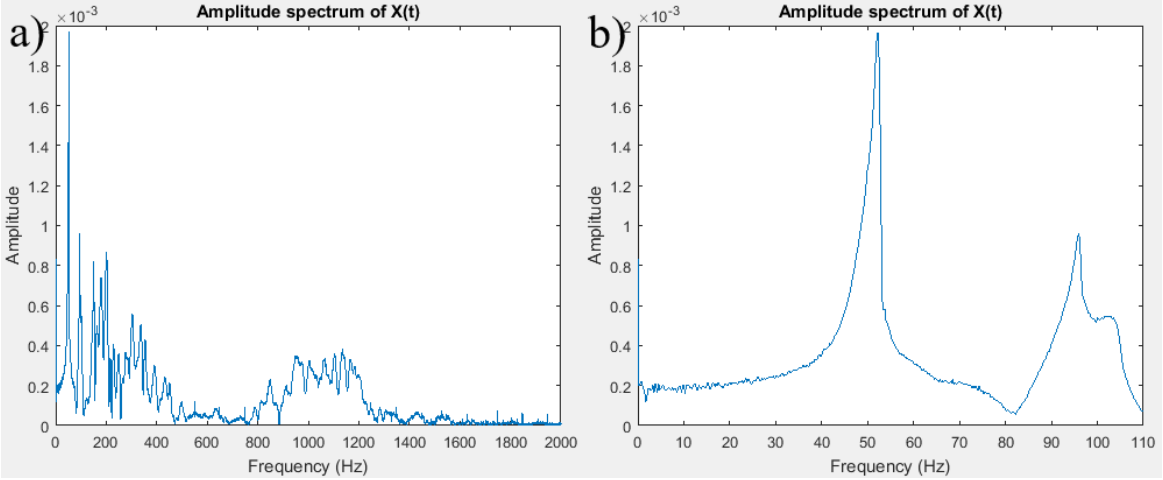

Figure 32. Measured amplitude spectrum from shaft with motor-measurement and it's zoom. a) is the amplitude spectrum to 2000 Hz and b) is a zoom of 0 – 110 Hz. We can see that the system is resonating at about 52 Hz, 96 Hz, 150 Hz, 200 Hz, and near several different spots on 1000-1200 Hz. *X*-axis are frequency in unit of Hz and *Y*-axis are amplitude of vibration in unit of m.

5 DISCUSSION AND CONLUSIONS

The done RoBeDyn-model is verified in this section with the measurement data from shaft only-measurement and from shaft with motor-measurement. After that, the results from test rig without SFDs are compared to results with SFDs. Then there is an analysis about the accuracy of done RoBeDyn-model and some investigation about factors that might affect into the accuracy of model. After that there is discussion about success of designing SFDs in this research. At the end, there are some suggestions for further research relating to this work.

5.1 Verification of results from RoBeDyn-model

For verifying the done numerical model, measurements from shaft with motor should match with results from that motor with shaft combinations Campbell diagram. We can see motor and shaft combinations natural frequencies collected up to 50 Hz from this configurations Campbell diagram in table 14. There are no SFDs in model. It is assumed that the effect of modal damping ratios is very small in this research.

Table 14. Natural frequencies from shaft with motor combinations Campbell diagram.

Mode	Rotation speed [RPM]	Frequency [Hz]
1	0	0.0
2	933	15.5
3	948	15.8
4	2843	47.8
5	2958	49.3

From figure 33, we can see the amplitude spectrum of motor and shaft-measurement, shown with results from shaft and motor combinations Campbell diagram. Modes above 50 Hz are not taken account, because the used electric motor cannot reach rotation speeds higher than 3000 RPM.

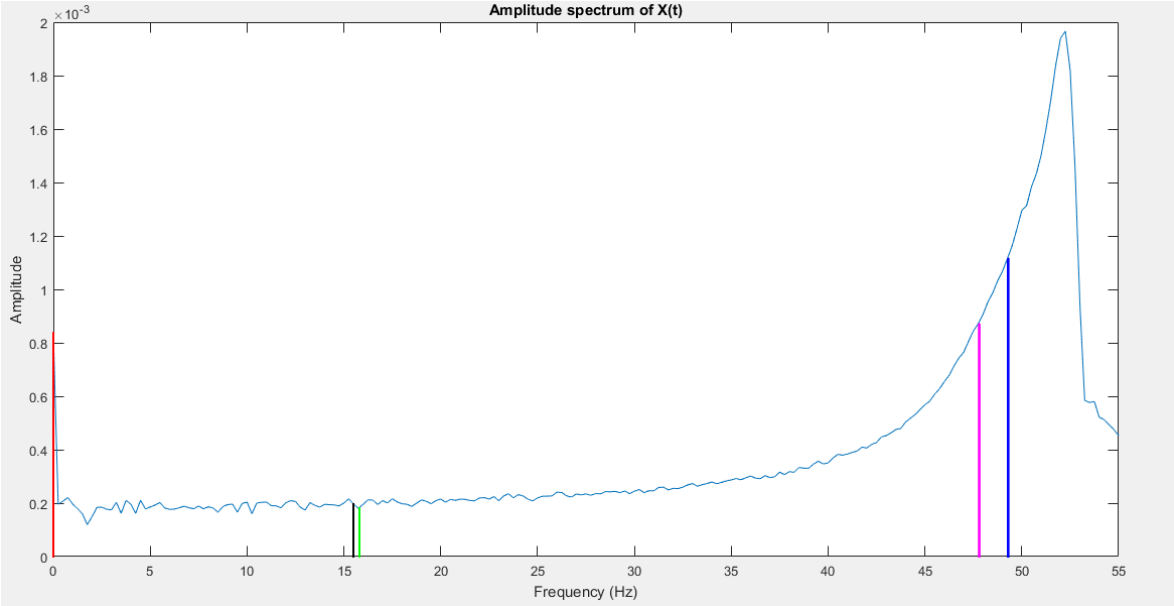

Figure 33. Amplitude spectrum of motor and shaft- measurement. The measured data is marked as blue and the red, green, black, magenta and dark blue lines are modes from Campbell diagram of shaft with motor combination from the RoBeDyn-model. Red line is mode 1, black line is mode 2, green line is mode 3, magenta line is mode 4 and dark blue is mode 5. *X*-axis is frequency in unit of Hz and *Y*-axis is amplitude of vibration in unit of m.

We can see that modes 4 and 5 are very near the resonance frequency of measured data. There is some inaccuracy on modes 4 and 5, because they are not exactly locating at the resonance spikes frequency. The higher vibration frequencies get, the higher an error in their values can get. We can see that modes 2 and 3 are not close resonance frequency of measured data. In measurements, the used impulse was relatively small and bearing houses' stiffness is very high. The response in measuring point, which happened to be the first bearing house, did stay very low for that reason. Also, by looking figures 26 and 27, we can see that in RoBeDyn-model there is displacement in model where bearing house is. But in real life, bearings do not allow displacement like in done model. By combining these two factors, 15.6 Hz is not having a resonance spike in measured data. Mode 1 is rigid body mode, which also is seen in measured data on 0.0 Hz frequency. The results of numerical model can be verified from this measurement of motor with shaft combination, because measured results were very close to results that numerical model was giving from measured situation.

We can see the free-free modes and natural frequencies from RoBeDyn-simulation with shaft only-simulation in table 15. There are no SFDs in model.

Table 15. RoBeDyn-results for free-free modes in shaft only-case.

Mode	Frequency [Hz]
1	30.12
2	30.12
3	70.20
4	70.21
5	111.4
6	111.4
7	224.6
8	224.6
9	263.0
10	263.0

From figure 34, we can see the amplitude spectrum of shaft only-measurement. Modes above 200 Hz are not taken account, because the inaccuracy in results can be growing too big, when frequencies get higher.

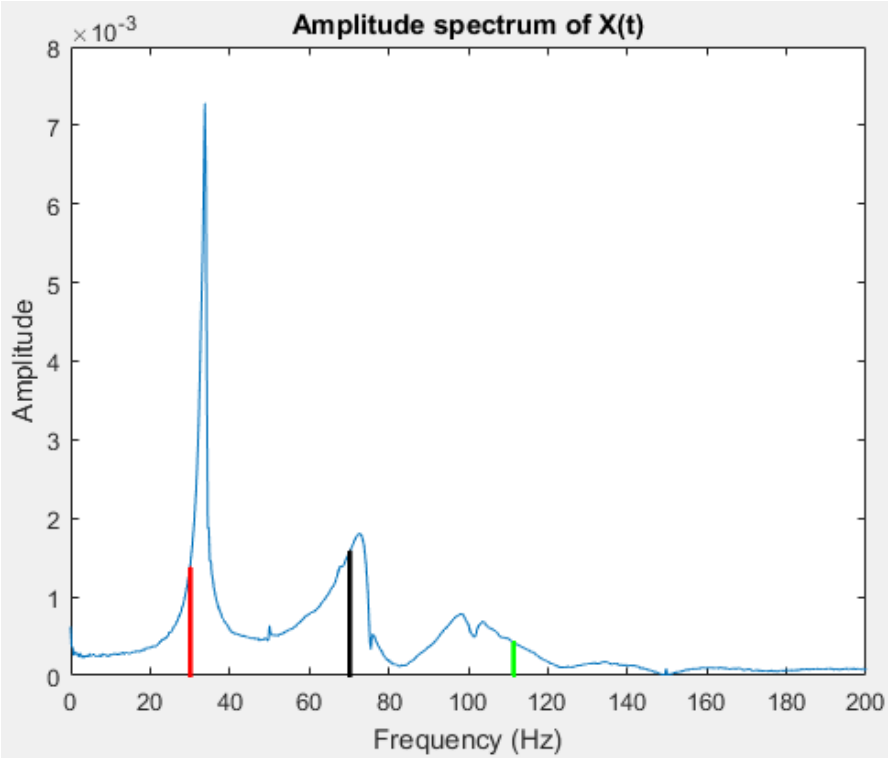

Figure 34. Amplitude spectrum of shaft only- measurement. The measured data is marked as blue and the red, green and black lines are free-free mode sets from the RoBeDyn-model.

Red line is modes 1&2, black line is modes 3&4 and green line is modes 5&6. *X*-axis is frequency in unit of Hz and *Y*-axis is amplitude of vibration in unit of m.

We can see that the system is resonating near those frequencies than there are listed in table 15. However, modes 5&6 are not that close resonance spike than modes 1&2 and 3&4 are. Modes 5&6 have some inaccuracy on them. The higher vibration modes get, the higher an error in their values will get. This might be the reason why modes 5&6 are not exactly locating in resonance frequency. The frequencies are at about 30 Hz, 70 Hz and 114 Hz. The numerical model can be verified from this measurement for the motor and shaft-combination.

5.2 Comparison of results without and with SFDs

In this section the results from the test rig without and with the designed SFD are compared to each other. The purpose of this comparison is to show how SFDs are affecting the dynamics behavior of test rig. All these results are from model with motor attached, because SFDs are useful only if rotor is rotating. Compared results without and with SDFs were unbalance response, Campbell diagram and whirling modes at resonance frequencies from test rig without SFDs.

5.2.1 Unbalance response comparison

We can see the unbalance response plots from the test rig without and with SFDs in figure 35.

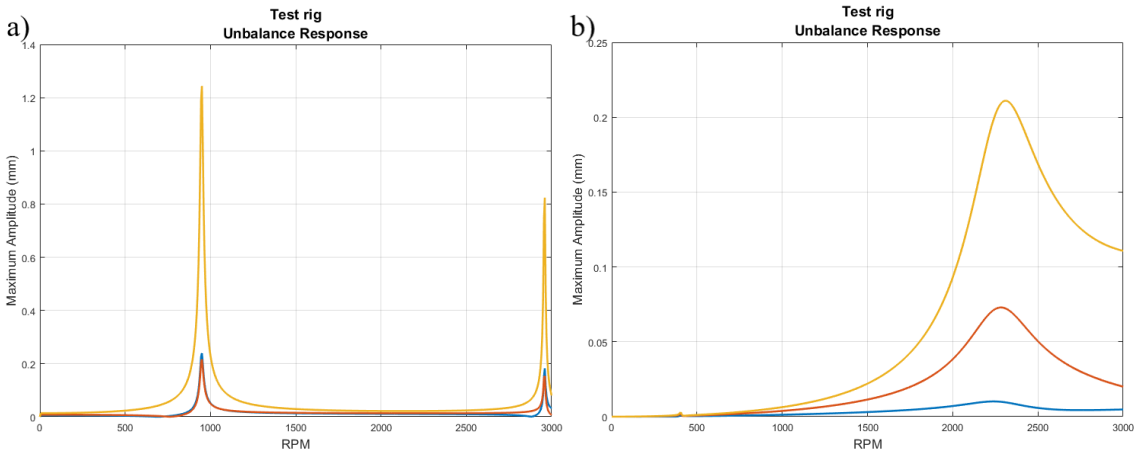

Figure 35. Unbalance response plots without and with SFDs. a) is without SFD and b) is with SFDs.

In figure 35, node 4 is marked as yellow and it is locating where the first weight disc, starting from the motor, is locating. Node 9 is marked as orange and it is locating where the second weight disc, starting from the motor, is locating. Node 21 is marked as blue and it is locating where shaft free end is locating. *X*-axis are rotation speed in unit of RPM and *Y*-axis are amplitude in unit of mm. We can see from the figure 35 that SFDs are lowering the maximum amplitudes dramatically and they are spreading the resonance spikes on wider range of rotational speed. We can see that the dampers are damping vibrations as expected. The decrease in vibration amplitude is clearly caused by SFD's damping, because the test rig itself has only modal damping and it is insignificantly small compared to the SFD's damping. This effect can be seen in from lowering the maximum amplitude from 1.24 mm (without dampers) to 0.21 mm (with dampers).

5.2.2 Campbell diagram comparison

We can see the Campbell diagrams from test rig without and with SFDs in figure 36.

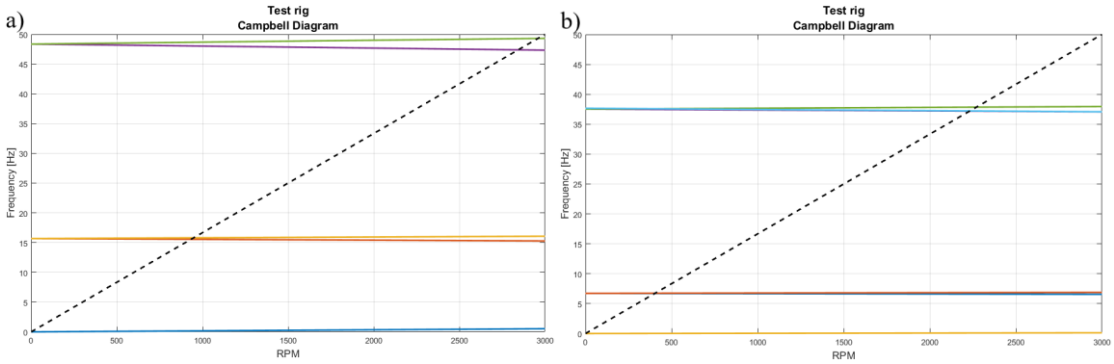

Figure 36. Campbell diagrams without and with SFDs. a) is without SFDs and b) with SFDs. *X*-axis are rotation speed in unit of RPM and *Y*-axis are frequency in unit of Hz.

We can see from the figure 36, that the SFDs are affecting Campbell diagram, by lowering the frequencies of modes. We can see that on Campbell diagram with SFDs, there is a rigid body mode (Shabana 1989, p. 335-336). Rigid body mode can be seen marked on blue on a) and on yellow on b) at the figure 36. In common, SFDs seem to bring the different modes on lower rotational speeds. SFDs modelled with mass insignificantly small compared to the total mass of rotor, so the change in systems stiffness due to the SFD spring could be the reason what makes resonance frequencies getting to lower rotation speeds.

5.2.3 Whirling mode comparison with and without dampers

Whirling modes of test rig without and with SFD are compared here. The variables that we are interested are frequency for modes, type of whirling and damping ratio at different modes. We are interested only from four first whirling modes of test rotor, because modes higher than 50 Hz, cannot be exited with test rigs motor. The test rig without SFDs was resonating at 950 RPM and at 2960 RPM, so we are using these speeds for comparison. Whirling mode's data at 950 and 2960 RPM can be seen in table 16.

Table 16. Whirling modes data with and without SFD at 910 and 2160 RPM. Forward modes are marked as FW and backward modes are marked as BW.

	No SFD	With SFD	No SFD	With SFD
	@ 950 RPM	@ 950 RPM	@ 2960 RPM	@ 2960 RPM
Mode	*f* [Hz]	*f* [Hz]	*f* [Hz]	*f* [Hz]
1	0.1671 (FW)	6.67 (BW)	0.5702 (FW)	6.56 (BW)
2	15.55 (BW)	6.772 (FW)	15.29 (BW)	6.88 (FW)
3	15.81 (FW)	0.03927 (BW)	16.07 (FW)	0.122 (BW)
4	48.04 (BW)	37.38 (BW)	47.35 (BW)	37.07 (BW)

	No SFD	With SFD	No SFD	With SFD
	@ 950 RPM	@ 950 RPM	@ 2960 RPM	@ 2960 RPM
Mode	Damping ratio [%]	Damping ratio [%]	Damping ratio [%]	Damping ratio [%]
1	0.000	1.04	0.000	1.03
2	0.98	1.06	0.979	1.07
3	0.98	100	0.980	100
4	0.149	8.32	0.149	8.13

We can see from table 16, that rotors first mode without SFDs on 950 RPM is almost 0 Hz. SFDs are changing the third mode on 950 RPM very near 0 Hz and raising first modes frequency. We can see from table 16, that the first mode is reached at almost 0 Hz on 2960 RPM at rotor, when there are no SFDs. In this case too, SFDs are lowering the third mode into almost 0 Hz and raising the first modes frequency. The change in modes might be

happening because, damping ratio at third mode on both cases, is increasing about 100 %. Damping ratio increases on all modes, because SFDs are designed to raise systems damping.

On modes 2, 3 and 4 in both cases, we can see that SFDs did lower modes frequencies. That might be happening because damping on those modes is rising and more vibration energy is being absorbed by designed dampers. However, in both cases, because of mode 1 changing from rigid body mode to lateral bending mode, its frequency with SFDs is rising. This might be happening, because on both cases, SFDs are turning mode 3 to rigid body mode. SFDs had some effect on the types of whirling modes on both cases. SFDs changed on modes 1, 2 and 3 backward whirling modes to forward whirling modes and vice versa. However, on mode 4, there was not that kind of effect. That might be happening, because fourth mode is not that robust to change in type of whirling or the error in model is growing high enough on fourth mode.

5.3 Accuracy of the model

We can see that measured data and the done RoBeDyn-model have some difference in gained results. The difference to the results can be coming for example from these sources:

- Modal damping ratios for modes 1-6 are estimated fixed constants in RoBeDyn model. In real life, they are most likely not same constants or constants at all, than the ones used in RoBeDyn-model. There is no modal damping for modes 7-10 in RoBeDyn-model. In real life there is a little damping on those modes too. The damping in components and joints is not taken account in RoBeDyn-model. In real life, the joints and components have a little damping effect on them.
    - On this research, seemed that the modal damping's did not have almost any effect on the results.
- Material and its homogeneity could be one factor. In RoBeDyn-model all components are done from same material with same elastic modulus and density. In the test rig the material is not same for all components and there can be inhomogeneity in material.
- The accuracy for locating the components in the test rotor: accuracy for measuring the locations for components was ±5 mm.

- The mass of unbalanced mass in weight discs was very difficult to estimate. There was unbalance in discs even without any weight bolts. This unbalance was caused from inaccuracy in manufacturing processes and from the welding process.
- Bearings are assumed to be almost massless in made RoBeDyn-model. The mass of bearing was small compared to the total mass of other components. Also, only the inner core and rolling elements would be spinning while rotor is operating. This would make bearings mass in rotor even smaller.
    - SFDs are attached into the bearings, but the SFDs are modelled almost massless, because SFDs are not rotating. The mass of SFDs is insignificantly small compared to the total mass of rotor.
- There is no friction added in RoBeDyn-model, for example there would be some friction in bearings and on their roller elements, which might be big enough to affect the results.
- Stiffness of ROTEX-joint is not very accurate. ROTEX consists from three different components, but in this case, they are modelled as one component. The stiffness of ROTEX-joint is higher in model than it would be in real-life.
    - ROTEX is also made from aluminum, which is not taken account in RoBeDyn model. In RoBeDyn model ROTEX is modelled to be same material than other components are.
- Stiffness on other components are only base on calculational data of rigs components. It does not take account any special features in components geometry such as holes or complex geometry. This will effect on stiffness of components and cause some error in RoBeDyn model's results compared to measured data. Stiffness is one of main factors to systems natural frequencies.

5.4 Success of design of SFDs

Demand was to have same stiffness in *Y*- and *Z*-direction and damping in *Y*- and *Z*-direction. This demand was fulfilled, because in designed SFDs values for stiffness in *Y*- and *Z*-direction and for damping *Y*- and *Z*-direction are equal. The stiffness in *Y*- and *Z*-direction is 388.8 N/mm and damping in *Y*- and *Z*-direction is 2024 Ns/m. One of the demands was to design SFDs so that they are modular unit. SFDs were designed as ISFD, which makes designed SFD modular units. Designed SFDs can be fitted around bearing and they are easy to assemble and disassemble. Some of the demands were, that designed SFD needed to have

inner diameter of 62 mm and thickness of 14 mm maximum. On designed SFD, these demands were taken account. Designed SFD inner diameter is exactly 62 mm and the thickness is 14 mm. Last demand for SFD design was that SFDs stiffness-damping ratio needs to be designed so that SFDs are dramatically lowering vibrations in test rotor. This demand was fulfilled by adjusting stiffness-damping ratio in designed SFDs so, that they lowered maximum amplitudes about 83.0%. Because of the lack of space for SFDs in bearing houses, there was a wish for design that SFDs outer diameter can be 71.5 mm maximum. In designed SFDs the outer diameter was 68.0 mm, so this wish was fulfilled. SFDs were designed using SolidWorks, which is a 3D-modelling software, so there exists 3D-model of designed SFD. Other of the wishes for design was to have 3D-model of designed SFDs.

Things pointed out in this section are showing that the designed SFD is supporting modular design theory. The SFDs were designed so, that they do not have need for oil pump. It is assumed that SFDs are not leaking their oil out. When SFDs get worn out too much, new pair of SFDs can be easily assembled into bearing houses. This is supporting modular design, because adding an oil pump and oil supply lines for SFDs would have changed the design process much and would have been doing modular designing much harder. Oil pump and oil supply lines most likely would have needed usage of different bearing houses too. SFDs were designed as modules, so they can be easily assembled or dissembled from test rig. Also, other modular units with same physical size than designed SFDs, but different properties, such like damping or stiffness, can be fitted into test rig instead of SFDs. This way properties of test rig can be adjusted just by changing modular units. (Säilynoja 2014, p. 34-36).

5.5 Sensitivity, reliability and validity of numerical model

By looking done numerical models' sensitivity, the done numerical model relies mostly on mass of the components, their mass momentums in *X*-, *Y*- and *Z*-direction, their stiffness and their location global coordinate system in model. Small scale changes in input parameters seemed not to have that big enough effect on gained results, but the big changes in input parameters effect the systems natural frequencies and behavior.

By looking into done numerical models' reliability, the done numerical model did not change the results, if input parameters were not changed. If input parameters for simulation run were

changed, the results changed too. However, in numerical model there were some problems too. There were some problems with whirling mode calculation. In done numerical model components, such as bearing, were not able to move or bend in realistic way on their supports. This caused some differences in results between measured data and between numerical model. But by combining knowledge from done measurements and from numerical model, problems like that can be detected and fixed, which will make the numerical model more reliable.

Done model is based on findings of rotor dynamics' and multibody system-modelling's literature. Out of these 27 references, 12 were books, 4 were company's www-sites, 3 were scientific articles, 3 were private emails, 1 was doctoral thesis, 1 was licentiate thesis, 1 was catalogue, 1 was manual and 1 was master's thesis. From scientific articles, all 3 were published in 2019, so they are new. Books used as references are a little bit older, 5 of books was released after 2000. Some of the older books were widely used, such like Shabana's or Goodwin's book. The web documents and private emails included only some specific data or specific models of test rig used in this research.

5.6 Further research

From continuing, where this research has ended, there would be some ideas for further research. First, making manufacturing plan for the SFDs and manufacturing them. Secondly, verifying the results in test rig with the manufactured SFDs and comparing the results to the RoBeDyn-results. There also would be further research about designing an assignment for learning about rotor dynamics, doing measurements from rotor system and for modelling the test rotor in modelling software.

6 SUMMARY

The test rig is an AMB-test rig and it was created originally for testing magnetic bearings and location sensors in RAMBO-project. On this research, the aim was to numerically model the test rig, find required parameters for designing SFDs, design squeeze film dampers as modular unit for test rig and study the behavior of test rig with designed SFDs. The challenge was the very small space in bearing housings for SFDs and lack of knowledge about modelling parameters for SFDs.

RoBeDyn-toolbox is numerical modelling toolbox in MATLAB for modelling dynamic rotor-bearing-systems and for visualizing gained results. RoBeDyn-model of test rig has following components modelled on it: shaft, bearings, bearing bushings, electric motor, ROTEX shaft coupling and weight discs. Also, the SFDs were added later into the model. The done RoBeDyn-model with SFDs has 21 elements and 23 nodes. Data about components for RoBeDyn-modelling was gained from the SolidWorks-model of test rig and some data was gained from done measurements with test rig. Done RoBeDyn-model was verified with data that was gained from done vibration measurements of test rig. Measurements were done with 1D acceleration sensors from two different cases: with motor attached and without motor attached into test rig. Both sets of measurements matched with results from done model.

By studying the behavior of RoBeDyn-model of test rig without and with the SFDs, the optimal parameters for SFDs stiffness, damping and dimensions were found. It was clear from the gained results, that with certain parameters the amplitude of vibration in resonance was at minimum value. These values and knowledge about demanded features for SFDs were used for designing SFDs in SolidWorks. In SolidWorks, there were several designed SFD-models. The SFD with closest parameters to the wanted values, was model with four springs and with two separate oil films with thickness of 0.27 mm. The required modelling parameters and their numerical values are listed in table 17. With parameters listed in table 17, SFDs could be designed as ISFDs and they could be added as modular units in the test rig.

Table 17. Parameters and their numerical values for designing SFDs.

Feature	Parameter	Unit
Inner diameter (d_{in})	62	mm
Outer diameter (d_{out})	68	mm
Length (L)	14	mm
Amount of springs (n)	4	-
Radius of first oil film (R_1)	32	mm
Radius of second oil film (R_2)	33	mm
Thickness of oil films (c_c)	0.1	mm
Damping (C_{SFD})	2024	Ns/m
Stiffness in Y-direction (k_{SFDy})	$388.8 \cdot 10^3$	N/m
Stiffness in Z-direction (k_{SFDz})	$388.8 \cdot 10^3$	N/m

By comparing numerical models unbalance response plots from test rig with and without SFDs, we found out that without SFDs, there were two clear resonance spikes in plot, but with SFDs the resonance spikes were divided into wider range of RPMs. Also, with SFDs, the maximum amplitude in all three tracked nodes was lowered dramatically. By comparing the RoBeDyn-model's Campbell diagrams from test rig without and with SFDs, we noticed that the SFDs are lowering the resonance frequencies. Figure of final version of designed SFD can be seen in figure 37.

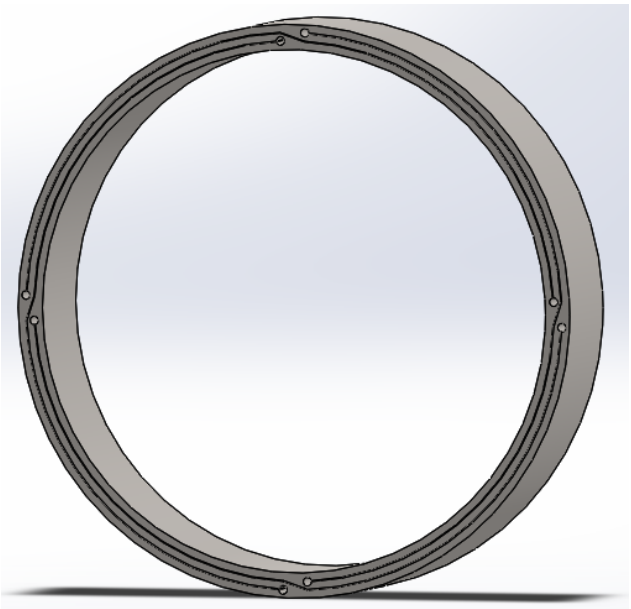

Figure 37. Final version of designed SFD.

LIST OF REFERENCES

Airila, M & al. 1985. Koneenosien suunnittelu 4. WSOY. p. 320-321.

Amirouche, F. 2006. Fundamentals of multibody dynamics. Birkhäuser. p. 321-322.

Beckwith, T., Buck, N. & Marangoni, R. 1982. Mechanical measurements. Third edition. p. 106-108.

Burton, T. D. 1994. Introduction to dynamic system analysis. McGraw-Hill, Inc. p. 595-599.

Dankowicz, H. 2005. Multibody mechanics and visualization. Springer. p. 368-376.

Friswell, I., Penny, T., Garvey, D. & Lees, W. 2010. Dynamics of rotating machines. Cambridge University Press.

Genta, C. 2005. Dynamics of rotating systems. Springer.

Goodwin, M. 1989. Dynamics of Rotor-Bearing Systems. Unwin Hyman Ltd.

Larsonneur, R. 1990. Design and control of active magnetic bearing systems for high speed rotation. Doctoral thesis. Swiss Federal Institute of Technology. p. 1.

Lu, K. & al. 2019. Experimental study on vibration suppression of gear shaft misalignment with ISFD. Scientific article. Beijing Key Laboratory of Health Monitoring and Self-Recovery for High-End Mechanical Equipment, Beijing University of Chemical Technology.

Meesus, H. & al. 2019. Dynamic Performance of an Oil Starved Squeeze Film Damper Combined with a Cylindrical Roller Bearing. Scientific article. Department of Mechanical Engineering, Vrije Universiteit Brussel.

Nässelqvist, M. 2009. Simulation and Characterization of Rotordynamic Properties for Hydropower Units. Licentiate thesis. Luleå University of Technology. p. 3.

Pfeiffer, F. 2008. Mechanical system dynamics. First edition. Springer. p. 6-8.

Shabana, A. 1989. Dynamics of multibody systems. A Wiley-Interscience Publication. p. 335-336.

Sikanen, E. 2019a. Funet FileSender: Rambo sisältöraportti. [Private e-mail message]. Receivers: Topias Parviainen. Sended: 2.5.2019 13:17 (GMT +0200).

Sikanen, E. 2019b. VL: Rambo test rig viimeisin SW malli. [Private e-mail message]. Receivers: Eero Scherman, Topias Parviainen. Sended: 2.5.2019 13:00 (GMT +0200). Attachment: "S126989.zip".

Sikanen, E. 2019c. Test rigin tietoja. [Private e-mail message]. Receivers: Eero Scherman, Eerik Sikanen. Sended: 27.5.2019 14:55 (GMT +0200). Attachment: "20190522_150431.jpg".

SKF. 2019. Deep groove ball bearings. [Company's www-site]. [Referred 14.8.2019]. Available: https://skf-preview-e.partcommunity.com/3d-cad-models/6007-z-skf?info=skf%2Fbearings_units_and_housings%2Fball_bearings%2Fdeep_groove_ball_bearings%2Fbb1_001_101.prj&cwid=2204

Sopanen, J. & al. 2019. RoBeDyn v.2.2 Theory Manual. [Manual]. [Referred 12.11.2019].

Stone, R. 1997. Towards a theory of modular design. The university of Texas at Austin. p. 17-18. [Referred 22.8.2019]. Available at: http://citeseerx.ist.psu.edu/viewdoc/download?doi=10.1.1.111.3841&rep=rep1&type=pdf

Säilynoja, P. 2014. Modulaarisen tuotteen mallivalikoiman ja tuotantorakenteen keventäminen. Master's Thesis. Lappeenrannan teknillinen yliopisto. p. 34-36.

VEM MOTOR. 2017. Standard motors. [Catalogue]. [Referred 19.9.2019]. Available: https://www.vem-group.com/fileadmin/content/pdf/Download/Kataloge/Kataloge/Hauptkatalog_2017_KAP2_en.pdf

Waukesha Bearings. 2019a. Fluid Film Solutions. [Company's www-site]. [Referred 11.6.2019]. Available: https://www.waukbearing.com/en/technical-resources/faqs/?ID=5

Waukesha Bearings. 2019b. ISFD® Integral Squeeze Film Damper. [Company's www-site]. [Referred 11.6.2019]. Available: https://www.waukbearing.com/en/engineered-fluid-film/product-lines/isfd(r)-integral-squeeze-film-damper/

Waukesha Bearings. 2019c. ISFD® Technology Integral Squeeze Film Damper Solution to Control Vibrations. [Company's www-site]. [Referred 11.6.2019]. Available: https://www.waukbearing.com/includes/systems/docs/loadFile.php?FID=4f15659cf1f0a5d70a7f94587f156879&download

Yamamoto, T. & Ishida, Y. 2001. Linear and nonlinear rotordynamics. Canada: John Wiley & Sons, Inc.

Zapoměl, J., Ferfecki, P. & Forte, P. 2019. Vibrations attenuation of a Jeffcott rotor by application of a new mathematical model of a magnetorheological squeeze film damper based on a bilinear oil presentation. Scientific article. Department of Dynamics and Vibration, Institute of Thermomechanics, The Czech Academy of Sciences, Dolejškova.

INDATA_Jeffcott.m.

```
% INPUT FILE FOR ROTOR-BEARING DYNAMICS CODE (RoBeDyn)

%-Model name------------------------------------------%
Inp.model_title='Test rig';

% akselin halkaisijat
D1=12.0*1e-3;    % akselin halkaisija

% Materiaaliarvot
E=2.1e11;
nuxy=0.3;
rho=7800;
ks=6*(1+nuxy)/(7+6*nuxy); %shear correction factor

%-Real Constant---------------------------------------%
%--ID,A,Izz,Iyy,H,B,theta,istrn,Ixx,shearz,sheary
Inp.Real=[ 1, pi*D1^2/4, pi*D1^4/64, pi*D1^4/64, D1, D1, 0, 0, pi*D1^4/32, ks, ks %akseli D1
            ];

%keypointit
k1=[0,0,0]'; % alku
k2=[1,0,0]'; % loppu

%-----------------------------------------------------------
% Solmujen ja elementtien generointi keypointtien välille.....
% [Node,Elem,MaxNodeNro,MaxElemNro]=
%                     Lmesh(startp,endp, Nelem,  MatID,RealID,   nodestart,elemstart,start_node)
[Node1,Elem1,MxN,MxE]=Lmesh(k1,k2         ,20,        1,1,               1,  1,1);   % shaft

%-Nodes-----------------------------------------------%
%-----ID,   X,   Y,   Z
Inp.Node=[Node1]; % kootaan node matriisi
for ii=1:1; eval(strcat('clear Node', num2str(ii))); end % tuhotaan turhat muuttujat

% Adding new nodes for SFDs
Inp.Node = [Inp.Node;
    22 0.2 -0.00 0
    23 0.7 -0.00 0
    ];

%-Elements--------------------------------------------%
%------ID, I,  J, Mat, Real
Inp.Elem=[Elem1
    ];
% kootaan Elem matriisi
for ii=1:1; eval(strcat('clear Elem', num2str(ii))); end % tuhotaan turhat muuttujat

%-Rajoitteet------------------------------------------%%-----Node, Dof, Value
% Dir 1=X, 2=Y, 3=Z, 4=RotX, 5=RotY, 6=RotZ
Inp.Disp=[1, 1, 0
          1, 4, 0
          2, 1, 0
          2, 4, 0
          3, 1, 0
          3, 4, 0
          4, 1, 0
          4, 4, 0
          5, 1, 0
          5, 4, 0
          6, 1, 0
          6, 4, 0
          7, 1, 0
          7, 4, 0
          8, 1, 0
          8, 4, 0
          9, 1, 0
          9, 4, 0
          10, 1, 0
          10, 4, 0
          11, 1, 0
          11, 4, 0
          12, 1, 0
          12, 4, 0
          13, 1, 0
          13, 4, 0
          14, 1, 0
          14, 4, 0
```

```
          15, 1, 0
          15, 4, 0
          16, 1, 0
          16, 4, 0
          17, 1, 0
          17, 4, 0
          18, 1, 0
          18, 4, 0
          19, 1, 0
          19, 4, 0
          20, 1, 0
          20, 4, 0
          21, 1, 0
          21, 4, 0

          22, 1, 0
          22, 4, 0
          22, 5, 0
          22, 6, 0

          23, 1, 0
          23, 4, 0
          23, 5, 0
          23, 6, 0
      ];

% Inp.Disp=[];
%-PointMass Elements-------------------------------------%
% Pistemassojen inertiat määritelty globaalissa koordinaatistossa
% MassPoints=   [ID, node, mass,    Jxx,        Jyy,        Jzz,        h,        L,     dia,   dia_in];
Inp.MassPoints=[ 1,   4,   1.69,    0.0038958,  0.0019907,  0.0019890,  0.025,    0.01,  0.150, 0;
                 2,   9,   1.69,    0.0038958,  0.0019907,  0.0019890,  -0.02,    0.01,  0.150, 0;
                 3,   1,   0.1345,  2.5780e-5,  2.5040e-5,  2.4860e-5,  0.032,    0.064, 0.041, 0.012;
                 4,   5,   0.6996,  0.00015204, 0.0013135,  0.00131353, 0.04495,  0.127, 0.041, 0.012;
                 5,   15,  0.6996,  0.00015204, 0.0013135,  0.00131353, -0.04495, 0.127, 0.041, 0.012;
                 6,   1,   4.90,    0.00013,    0.00005,    0.00005,    -0.0912,  0.178, 0.118, 0.00;
                 7,   22,  0.10877, 0,          0,          0,          0,        0.014, 0.062, 0.0715;
                 8,   23,  0.10877, 0,          0,          0,          0,        0.014, 0.062, 0.0715
                 ];

%-SpringDamper ------------------------------------------%
kSFDY=0%388.8e3 % 4 jousinen %200e3 oli paras
kSFDZ=0%388.8e3 % 4 jousinen %200e3 oli paras

myy1=142.2e-3; % Viskositeetti
R1=32.0e-3; % Säde
L1=14e-3; % Pituus
cc1=0.27e-3; % Kalvon paksuus

myy2=142.2e-3;
R2=33.0e-3;
L2=14e-3;
cc2=0.27e-3;

CSFD=0%(pi*myy1*R1*L1^3)/(2*cc1^3)+(pi*myy2*R2*L2^3)/(2*cc2^3) % 2000 oli aika hyvä

cSFDY=CSFD;
cSFDZ=CSFD;
%   SpringDamper=[ID, Inode, Jnode, Type, Dir,  Value];
Inp.SpringDamper=[1, 22, 0, 1, 2, kSFDY; % etu SFD Y %Inode 22
                  2, 22, 0, 1, 3, kSFDZ; % etu SFD Z %Inode 22
                  3, 22, 0, 2, 2, cSFDY; % etu SFD Y %Inode 22
                  4, 22, 0, 2, 3, cSFDZ; % etu SFD Z %Inode 22

                  5, 23, 0, 1, 2, kSFDY; % taka SFD Y %Inode 23
                  6, 23, 0, 1, 3, kSFDZ; % taka SFD Z %Inode 23
                  7, 23, 0, 2, 2, cSFDY; % taka SFD Y %Inode 23
                  8, 23, 0, 2, 3, cSFDZ; % taka SFD Z %Inode 23
                 ];

% Type = 1 --> spring
% Type = 2 --> damper
% Dir 1=X, 2=Y, 3=Z, 4=RotX, 5=RotY, 6=RotZ.
% Jos J node on 0, niin jousi on maassa kiinni

% Unbalance masses----------------------------------------
% -- Node, value (kg*m), angle
Inp.UB=[4, 0.25*4.08e-3*30e-3, 0;
        9, 0.25*4.08e-3*30e-3, 0;

];
```

```
%-Materiaali-------------------------------------------%
%---- ID, E, nuxy, rho
Inp.Mat=[ 1,  E, nuxy, rho
        ];
%-lumped massa, jos lumpm=1----------------------------%
Inp.lumpm=0;

% modal damping ratios
%                     Mode#, damping
Inp.ModalDamping=[ 1,    10*1e-3   %1. taivutus
                   2,    10*1e-3
                   3,    1.5e-3  %2. taivutus
                   4,    1.5e-3
                   5,    2e-3   %3. taivutus
                   6,    2e-3];



% Bearing parameters ------------------------------------%
if 1

    % Laakerin matriisien input-----------------------------------%
    jj=1;
    Inp.Bearing(1).type='Bearing Matrix'; % Stringi, joka kuvaa laakeria
    Inp.Bearing(1).Inode=5;     % Akselin solmu, johon laakeri on liitetty
    Inp.Bearing(1).Jnode=22;     % Tuennan solmu, johon laakeri on liitetty

    % Stiffness matrix (directions in global coordinate system, x=axial dir. yz=radial)
    %     Kb=[kxx  kxy  kxz
    %         kyx  kyy  kyz
    %         kzx  kzy  kzz];
    Inp.Bearing(1).Kb=[0    0       0
                       0    2e8       0
                       0      0     2e8];
    % Damping matrix (directions in global coordinate system, x=axial dir. yz=radial)
    %     Cb=[cxx  cxy  cxz
    %         cyx  cyy  cyz
    %         czx  czy  czz];
    Inp.Bearing(1).Cb=1e-5*Inp.Bearing(1).Kb;

    % Toinen laakeri
    Inp.Bearing(2)=Inp.Bearing(1);
    Inp.Bearing(2).Inode=15;     % Akselin solmu, johon laakeri on liitetty
    Inp.Bearing(2).Jnode=23;     % Tuennan solmu, johon laakeri on liitetty

    % Laakeri matriisi input loppuu--------------------------------%
else
    Inp.Bearing=[];
end

%-Lähtötietojen muokkaus parempaan muotoon---------------------%

% Lisätään massapisteet Elementti matriisiin indeksointia yms. varten
for jj=1:size(Inp.MassPoints,1)

    ElemMP(jj,1)=MxE+jj; % maksimielementtinumero +1
    ElemMP(jj,2)=Inp.MassPoints(jj,2); %Solmunumero
    ElemMP(jj,3:5)=0; % J node ja muut parametrit nollia

end
% Päivitetään
if exist('ElemMP')
    Inp.Elem=[Inp.Elem
        ElemMP];
end

%-Voimat-----------------------------------------------%
%-----Node, Dof, Value
% Force=[5,  1,   5000];
Inp.Force=[];

%-Cleanup----------------------------------------------------%
% Poistetaan väliaikaiset muuttujat
save ModelInp.mat Inp
clear all
load ModelInp.mat
%------------------------------------------------------------%
```

MAIN_Jeffcot.m.

```
% Simple Rotor with an overhung disk
% Rotor-Bearing Dynamic Analysis (RoBeDyn) Main Script
%
% ======================================================
clear all; close all;
for i=1:20; disp(' ');  end; clear i;
disp('Start of RoBeDyn Analysis'); disp(' ');


% PREPROCESSING.............................................................
% Read Input Data
INDATA_Jeffcott;  % Simple Jeffcott rotor, unsymmetric bearings

% Draw Model as a 3D WireFrame plot
f_RGeomPlotWireFr(Inp, [1 1 1 1 1], [0 1],{'-b',3});
view(2); axis equal; axis vis3d; view3d rot %figure settings

% END OF PREPROCESSING.....................................................

% % Free-free Modes^^^^^^^^^^^^^^^^^^^^^^^^^^^^^^^^^^^^^^^^^^^^^^^^^^^^^^^^
 Request.FreeModes.NroFreqs=10;      % Number of frequencies to be solved and plotted
 Request.FreeModes.PlotModes='Yes'; % Plot mode shapes 'Yes' or 'No'
% % Mode plotting options
% %                            Mode#, ScaleFactor, linetype, linewidth
 Request.FreeModes.ModePlot={1, 1000, '-k',  2
                             2, 1000, '--k', 2
                             3, 12000, '-r',  2
                             4, 12000, '--r', 2
                             5, 20000, '-g', 2
                             6, 20000, '--g', 2
                            };
 Request.FreeModes.Options={'view','XY',            % plot view. 'XY'=XY-plane, 'XZ'=XZ-plane, '3D'=3D
view
                            'originloc', [-0.3,0.0,0],% location of origin triad (default = [0,0,0]
                            'shading', 'on'         % wireframe or surface plot (default = wireframe)
                            'transparency',0.4      % transpacenrency of faces (0..1) if shaded plot
(default=1)
                            };
% % Calculate Free-Free Modes
 %% [FrqR,DampR,FiiR,Matrx]=f_FreeModes(Inp,Request)
[FrqR,DampR,FiiR,Matrx]=f_FreeModes(Inp,Request);

% End-of-free modes^^^^^^^^^^^^^^^^^^^^^^^^^^^^^^^^^^^^^^^^^^^^^^^^^^^^^^^^

% return


% CAMPBELL DIAGRAM++++++++++++++++++++++++++++++++++++++++++++++++++++++++++
Request.Campbell.NroFreqs=6;                    % Number of solved frequencies
Request.Campbell.Spin_vec=(0:20:3000)*2*pi/60; % Speed range
Request.Campbell.Type='Full';                   % Use 'Full' method to reduce system DOFs
Request.Campbell.PlotDamping='No';              % Plot damping ratios 'Yes' or 'No'
% Campbell diagram calculation and plotting
[FrqR,DampR,Matrx]=f_Campbell(Inp,Request);
% END OF CAMPBELL DIAGRAM+++++++++++++++++++++++++++++++++++++++++++++++++++

% UNBALANCE RESPONSE*******************************************************
Request.UBResp.Spin_vec=(0:5:3000)*2*pi/60;       % Speed range
Request.UBResp.OutputNodes=[4, 9, 21]; % List of Output Nodes

% Calculate and Plot Unbalance response of given nodes
[MaxAmp,U_vector]=f_UBResponse(Inp,Request);

% Plot Rotor Deformed Shape (Requires pre-calculated rotor response)
Request.RespPlot.Spin_speed=10000*2*pi/60;    % Rotation Speed for deformed shape plot
% Plot Rotor Deformed Shape at given speed
%f_RespShapePlot(Inp,Request,U_vector,MaxAmp,1,10000); %kommentoitu pois
% END OF UNBALANCE RESPONSE************************************************
```

```
% ROTOR MODE SHAPE PLOT=================================================
Request.ModePlot.Spin_speed=950*2*pi/60; % Rotation Speed for mode shape plot % 950 & 2960
Request.ModePlot.PlotGeom='Yes';           % Plot rotor geometry 'Yes' or 'No'
Request.ModePlot.Options={ 'originloc', [0.0,0.0,0],% location of origin triad (default = [0,0,0]
                          %'shading', 'off'          % wireframe or surface plot (default = surface)
                          'transparency',0.2       % transpacenrency of faces (0..1) if shaded plot
(default=0.1)
                          };
sf=[1e1 2e2 5e2 5e2]; %skaalauskertoimet eri muodoille. Ilman SFD: [1e1 2e2 2e2 5e2], SFD:llä: [1e1 2e2
5e2 5e2]
% Plot 4 first modes
for ii=1:4
    Request.ModePlot.ModeNro=ii;
    Request.ModePlot.ScaleFactor=sf(ii);
    % Calculate and Plot Mode Shape
    f_ModeShapePlot(Inp,Request);
end
clear ii
% END OF ROTOR MODE SHAPE PLOT=========================================
```